SYNTHESIS AND CHARACTERIZATION OF NUCLEOBASE-CONTAINING POLYELECTROLYTES FOR GENE DELIVERY

Eveline M. van der Aa

Thesis submitted to the faculty of the Virginia Polytechnic Institute and State University in partial fulfillment of the requirements for the degree of

Master of Science in Chemistry

Timothy E. Long (Committee Chair)
Theresa M. Reineke (Committee Member)
Robert B. Moore (Committee Member)

May 5, 2010
Blacksburg, Virginia

Keywords: nucleobase, polyelectrolyte, water-soluble, gene delivery, hydrogen bonding, electrostatic interactions

SYNTHESIS AND CHARACTERIZATION OF NUCLEOBASE-CONTAINING POLYELECTROLYTES FOR GENE DELIVERY

Eveline M. van der Aa

ABSTRACT

Wide literature precedence exists for polymers containing electrostatic interactions and polymers containing hydrogen bonding motifs, however the combination of electrostatic and hydrogen bonding interactions is not widely investigated in current literature. Polyelectrolytes containing hydrogen bonding groups are expected to exhibit properties of both classes of supramolecular interactions. A series of adenine- and thymine-containing PDMAEMA and *tert*-butyl acrylate copolymers were synthesized to investigate the effect of incorporating hydrogen bonding groups into a polyelectrolyte. Incorporation of the styrenic nucleobases significantly affected the solubility of these copolymers on aqueous solutions and showed salt-triggerability with higher contents of these groups. Polyelectrolytes are capable of binding and condensing DNA through electrostatic interactions with the negatively charged phosphate groups of the DNA backbone; however a high degree of cytotoxicity is also often observed for these gene delivery systems. The high level of cytotoxicity is attributed to high degree of cationic character for the polyplexes formed with these systems according to the proton-sponge hypothesis. One method of reducing the overall cationic character for these systems is incorporation of non-electrostatic binding mechanisms such as hydrogen bonding. A series of nucleobase-containing PDMAEMA copolymers were utilized in order to investigate the effect of incorporation of these groups on the cell viability, binding efficiency, and transfection efficiency of PDMAEMA.

Table of Contents

List of Figures

List of Tables

Chapter 1. Introduction to gene delivery and hydrogen bonding

1.1 Abstract

Currently the treatment of genetic disorders centers on the concept of gene therapy. Recent research efforts toward the design of non-viral gene delivery vectors focus largely on synthetic cationic polymers because of the inherent synthetic capability to fine tune these structures to obtain optimal transfection efficiencies. One key concern of gene delivery agents based on cationic polyelectrolytes is the high degree of cytotoxicity associated with the high transfection efficiencies achieved with these vectors. The correlation between gene delivery and cytotoxicity stimulated research on non-electrostatic interactions as a binding mechanism for polyplex formation. Research of polymers containing hydrogen-bonding motifs modeled after small molecule binding of the minor groove of double stranded DNA demonstrates efficient DNA binding of these vectors as well as to provide polyplex stability similar to that observed for those electrostatic interaction-based complexes. Non-viral gene delivery vectors possessing multiple binding mechanisms including electrostatic and hydrogen bonding interactions also demonstrated efficient gene delivery. Analysis of these vectors allowed for further investigation into the role of hydrogen bonding interactions in the design of a more effective gene delivery vector. The analysis also provided other key observations in gaining a better understanding of structure-property relationships of various synthetic vectors.

1.2 Introduction to non-viral gene delivery

Current research in the treatment of genetic disorders centers on the concept of gene therapy.[1-8] Genetic disorders originate from either a variation in the gene or a mutation in an individual's DNA.[1-3,5,8] A variation in the gene is simply a different form of the gene, while a mutation is an alteration of the gene[4]. Gene therapy is a method for fighting these disorders through the transfer of specific nucleic acid sequences previously identified as possessing the capability to alleviate the symptoms of a genetic disease.[1-12] Identification of these "therapeutic genes" is a critical component in the development of treatment methods based on nucleic acid therapeutics.[2-4,6,7,10,11] Completion of a working draft of the human genome allowed for a better understanding of genetic diseases through the identification of the specific DNA sequences that are related to particular diseases.[8] Identification of these "therapeutic genes" is only one of the many obstacles to overcome in the advancement of gene therapy.[1-8] A major barrier impeding the advancement of gene delivery efforts is the development of a gene delivery method that is efficient, non-toxic, and allows for targeting of specific cells.[9-12] Several types of non-viral gene delivery agents are the focus of intensive research efforts, including the design of synthetic polycations able to bind DNA through electrostatic interactions.[9-20] This class of transfection vectors shows great potential for gene therapy because of the ability to fine tune the structure yielding properties of the polymer appropriate for a viable gene delivery system.[10,11,16]

Cationic polymer vectors are promising candidates for gene delivery agents due to the synthetic flexibility to alter the polymeric structure in ways that optimize transfection efficiencies.[21-43] The basis of nucleic acid delivery vectors derived from cationic

polyelectrolytes is formation of a complex with plasmid DNA (pDNA) through electrostatic interactions between the positively charged polymer chain and negatively charged phosphate backbone of *DNA*.[29,32,36,39,41,42]

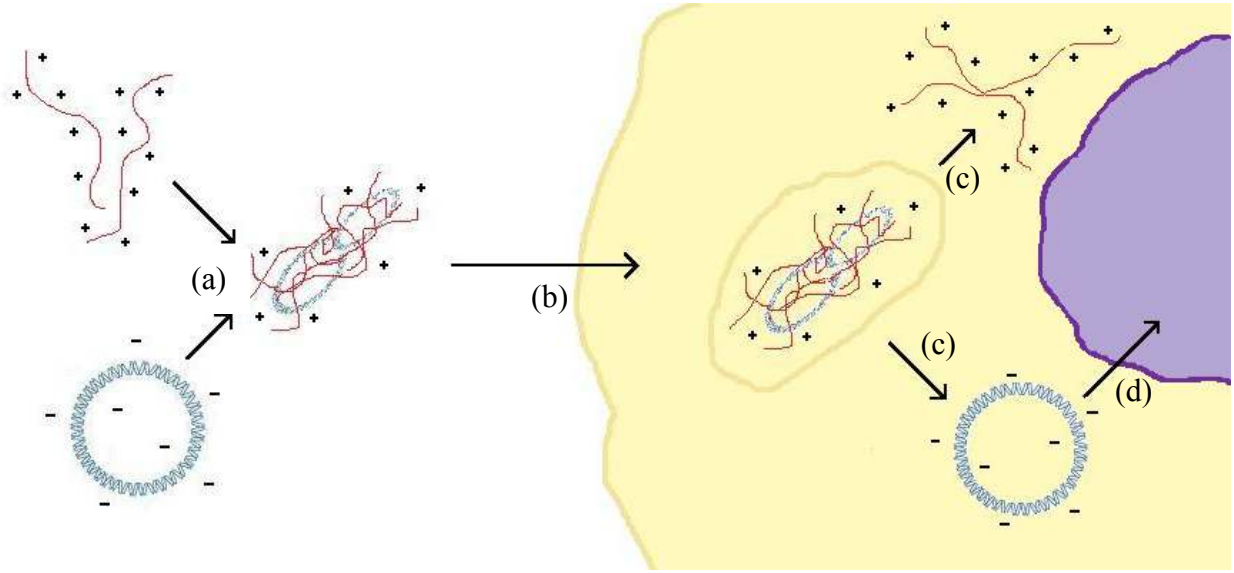

Figure 1.1. Scheme of polyplex formation and cellular uptake: (a) Effective binding and condensation of pDNA with cationic polyelectrolytes (b) Endocytosis of the polyplex (c) Polyplex dissociation (d) Nuclear uptake of uncomplexed pDNA

The process of gene delivery of these polyplexes undergo is outlined in Figure 1.1, beginning with the formation of the complex through electrostatic interactions and resulting in expression of the protein for which the pDNA is encoded.[11,39] These polymer-DNA complexes, known as polyplexes, range in size from approximately 30 to several hundred nanometers in diameter resulting from the condensation of pDNA through formation of the electrostatic interactions with polycationic molecules.[11]

The capability of the polymer to condense the DNA and to affect transfection efficiencies through the production of particle sizes appropriate for cellular uptake is essential for efficient gene delivery as well as protecting the pDNA from nucleolytic enzymes capable of degrading DNA fragments.[11] Mechanisms for the endocytosis of the

condensed particles include clathrin-mediated endocytosis (the only well-defined pathway), caveolae-mediated endocytosis, macropinocytosis, and clathrin and caveolae-independent endocytosis (Fig. 1.2).[44] The mechanism of endocytosis is dependent on a number of factors including the diameter of the polyplex and the cell type.[20,21,24-26,45,46]

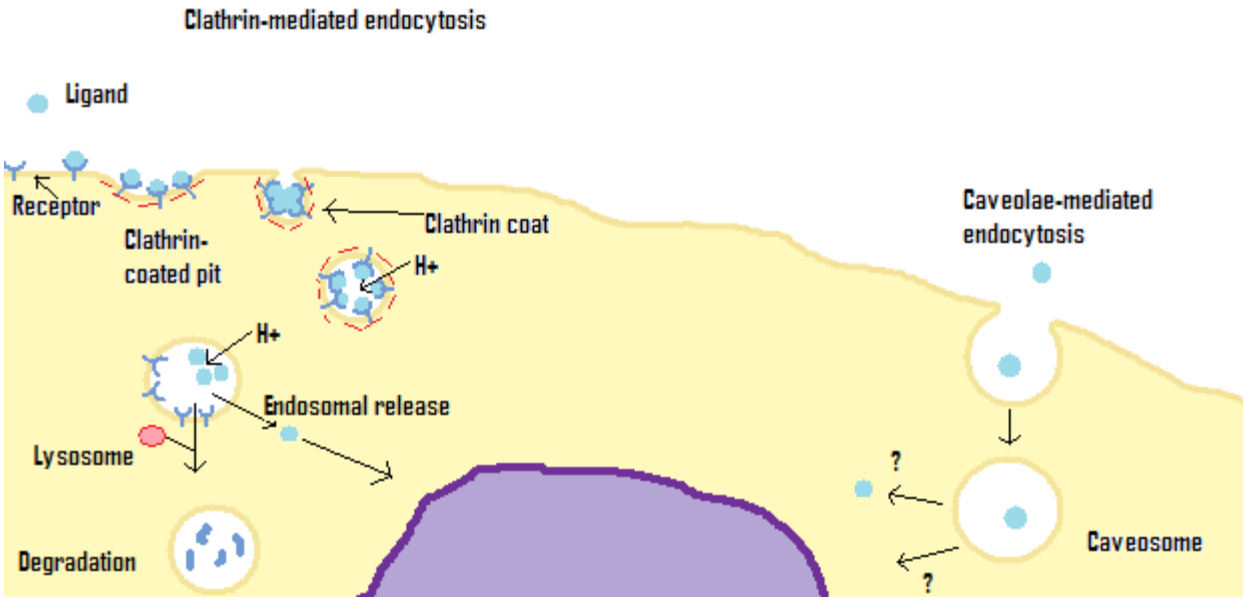

Figure 1.2. Clathrin-mediated and caveolae-mediated pathways of endocytosis[44]

Release of the particles and dissociation of the complexes must directly follow cellular uptake of the polyplexes.[9,10,18,20,47] It was hypothesized that the overall cationic character of the polyplex enables release from the endosomes preceding the dissociation of the interactions between the pDNA and polymer molecules.[15,20,47,48] The pDNA can then enter the porous nuclear membrane and subsequently expression of the encoded protein is observed.[11] Frequently high levels of cellular uptake are observed with little or no gene expression.[10] This is attributed to the inability of the polyplex to dissociate after cellular internalization since transcription factors of the host cell cannot effectively bind the pDNA while it remains bound to the cationic polyelectrolyte molecules.[10]

The structure of the cationic polyelectrolyte greatly influences the formation of the polyplex and sterically blocks the accessibility of the nucleolytic enzymes to the pDNA, which sterically blocks the accessibility of the nucleolytic enzymes to the pDNA structure and provides protection from degradation.[47] Formation of the polyplex results in a net positive charge for the condensed structure, which interact with negatively charged membrane components of the cell.[11,16,18] Plasmid DNA escape from endosomes is a vital step in the gene delivery process because release of the pDNA into the cellular cytoplasm must occur before nuclear translocation can transpire.[11,47] A key factor in low transfection efficiencies of polycationic gene delivery vectors is the inefficient release from the endosomes.[12] The polycation structure determines the binding strength of the polyplex, which affects the ability of the complex to dissociate allowing for nuclear translocation of the pDNA.[11,47]

Transfection studies of luciferase-encoded pDNA into COS-7 cells reveal a strong relationship between transfection efficiencies and the molecular weight of the polycation.[49] Layman et al. showed that gene expression increases significantly as a function of increasing molecular weight; however molecular weight was not shown to influence cellular uptake of polyplexes formed with these vectors.[50] Even though it was shown that condensed pDNA particles with a smaller average diameter were attained with high molecular weight PDMAEMA as compared to low molecular weight polymers, no correlation was shown with polyplex diameter and transfection efficiency.[49]

An experimental correlation exists between transfection efficiency and cytotoxicity of this gene delivery vector, both in its free form or bound in the polyplex, which is due to membrane destabilization upon cell entry.[19,49] Incorporation of groups

capable of non-electrostatic interactions with DNA in the polymer structure would decrease the cationic character of the vectors, which is hypothesized to minimize the cytotoxic effect observed for these polyplexes.[19] One non-electrostatic interaction under current investigation is hydrogen bonding of specific compounds to the major and minor groove of double stranded DNA. Structural features of the DNA double helix include the major groove and minor groove shown in Figure 1.3.

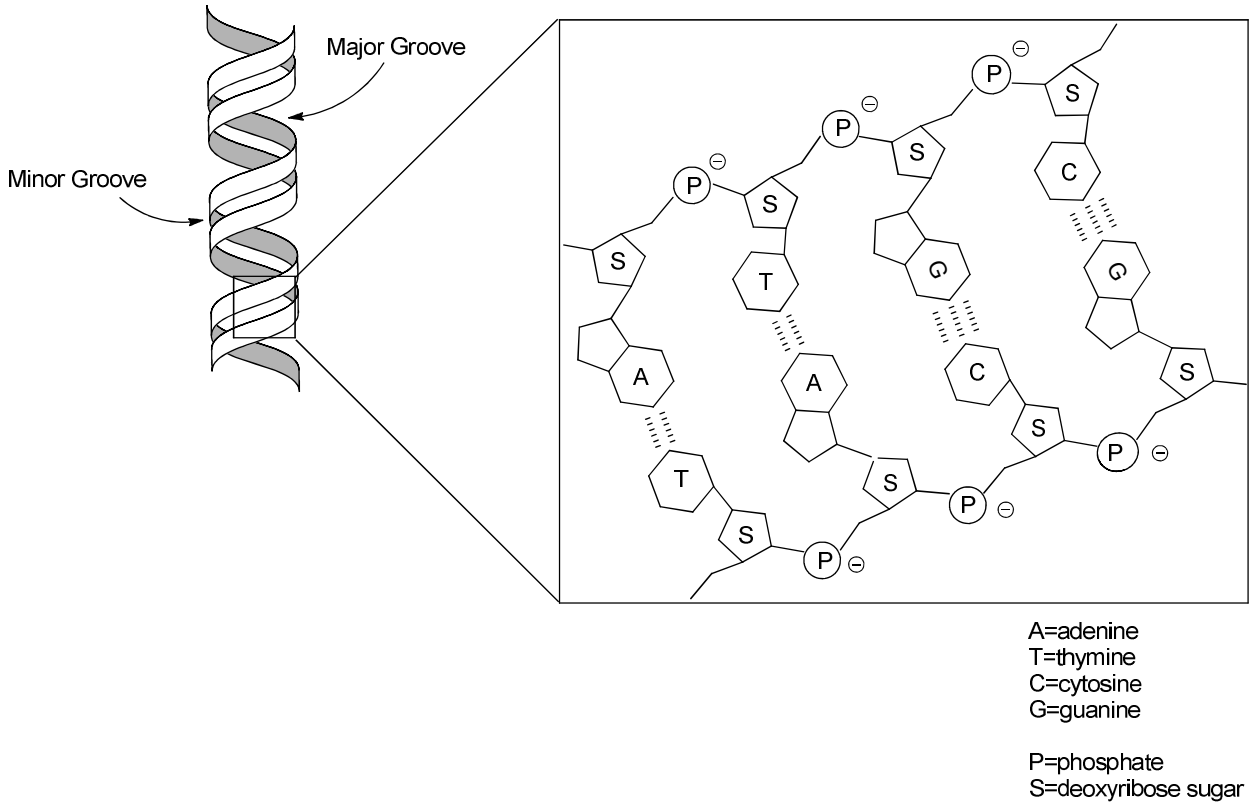

Figure 1.3. Double helix structure of DNA

Variation in the width of these two distinct indentations is attributed to the asymmetrical attachment of the nucleic acid base pairs to the phosphodiester backbone. The edges of the base pairs are exposed in these grooves act as both hydrogen bond donors and acceptors.[51] Hydrogen-bonded nucleic acid base pairs are primarily stabilized with electrostatic interactions. The nucleobase amino groups are both flexible and nonpolar, which allows for out of plane hydrogen bonding interactions to occur. [52]

1.3 Hoechst 33258 in gene delivery

2'-(4-hydroxyphenyl)-5-[5-(4-methylpiperazine-1-yl)benzimidazo-2-yl] benzimidazole (Hoechst 33258) is a fluorescent stain widely used to label DNA for fluorescence microscopy.[51,53,54] The benzimidazole group of this DNA binding agent is shown to form hydrogen bond interactions with the minor groove of helical double-stranded DNA (dsDNA).[19,54] Calorimetric and spectroscopic studies of the binding of the dication form of Hoechst 33258 to DNA oligonucleotides revealed two specific binding schemes defined as quasi-minor groove binding and stacked binding.[53,55] Quasi-minor groove binding is described as the binding of a single molecule to a minimum of 12 base pairs in contrast, stacked binding is predominately due to electrostatic interactions between the dication and the negatively charged phosphate backbone of DNA.[55]

Preliminary research evaluated a gene delivery agent capable of binding DNA though hydrogen bond interactions with Hoechst 33258.[19] Complexes formed from Hoechst 33258 and dsDNA showed no retardation of migration through electrophoresis gel as compared to naked DNA, suggesting that the complexed DNA is not in the compacted state typically observed in complexes based on electrostatic interactions.[19] These results are consistent with the hypothesis of a complex formed through hydrogen bonding interactions having conformation typical of its native form.[19] Further investigation of Hoechst 33258 based gene delivery vectors was accomplished using the dodecyl and octadecyl carbamate derivatives of Hoechst 33258 depicted in Figure 1.4.[19]

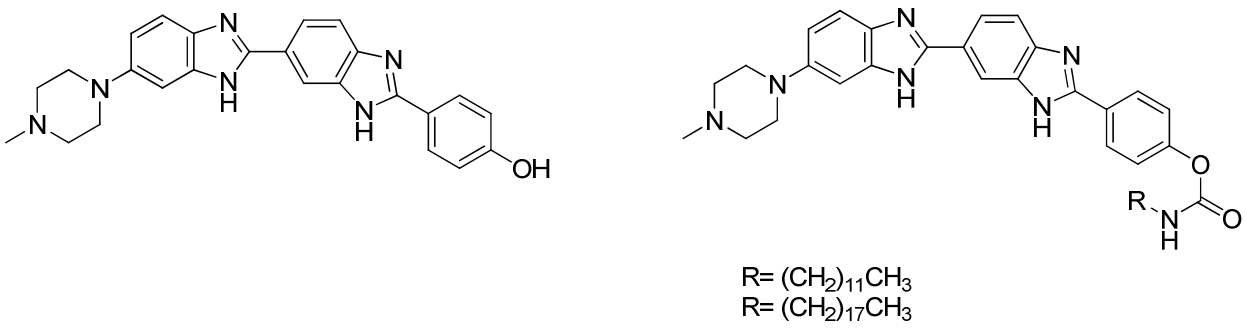

Figure 1.4. Hoechst 33258 and its alkyl derivatives.[19]

Comparison of fluorescence spectra of the two complexes with the spectrum of unbound Hoechst 33258 showed effective DNA binding.[19] Gel electrophoresis of the complexes showed similar results as unbound DNA unlike complexes of DNA and cationic lipids structurally similar to the Hoechst 33258 derivatives, which lead to compacted structures similar to cationic polymers.[19]

Utilizing the miscibility of the small molecule with poly(ethylene imine), incorporation of Hoechst 33258 into the polymer matrix allowed for further investigation into Hoechst 33258 s a gene delivery vector due.[15] Incubation of Hoechst 33258 with PEI:DNA complexes prior to transfection experiments showed higher gene expression than PEI-DNA complexes without incorporated Hoechst 33258.[15] Several pathways are hypothesized through which incorporation of Hoechst 33258 may increase PEI-mediated transfection efficiency, one of which is based on the ability of Hoechst 33258 to pass through the cellular membranes and promptly undergo nuclear uptake.[15] Incorporation of Hoechst 33258 into PEI:DNA complexes may alter the intracellular trafficking of these complexes, which may take on membrane-permeable characteristics similar to that of Hoechst 33258.[15] It was also hypothesized that Hoechst 33258 also facilitates nuclear targeting based on the observation of lower concentrations of these complexes in

endosomes and their nuclear localization.[15] Hoechst 33258 incorporated PEI:DNA complexes target the transcriptionally active sequences of DNA. This is attributed to the selectivity Hoechst 33258 shows for AT-rich DNA sequences since subnuclear positioning of DNA is shown as one of the mechanisms for the regulation of transcription.[15]

1.4 Hydrogen bonding interactions with nucleobases and gene delivery with PVDAT

Poly(2-vinyl-4,6-diamino-1,3,5-triazine) (PVDAT) is shown to bind nucleic acid bases through complementary hydrogen bond interactions with the binding strength proportional to the number of hydrogen bonds formed.[56-61] Neighboring hydrogen bonds contribute attractive or repulsive secondary interactions as depicted in figure 1.5 for triple hydrogen bonding arrays.[62]

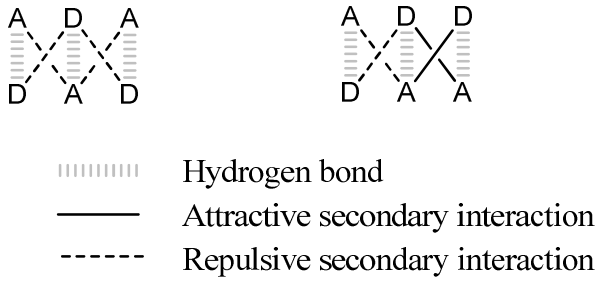

Figure 1.5. Secondary interactions in triple hydrogen bonding arrays

Hydrogen bond donors (or acceptors) in diagonally opposite sites result in secondary repulsive forces while a donor and an acceptor provide attractive forces.[63-67] In multiple hydrogen bonding arrays the binding motif DDD-AAA maximizes the number of attractive secondary interactions and gives the strongest overall interaction while the ADA-DAD binding motif yields a reduced strength for the overall interaction due to the maximized number of repulsive interactions.[63-68]

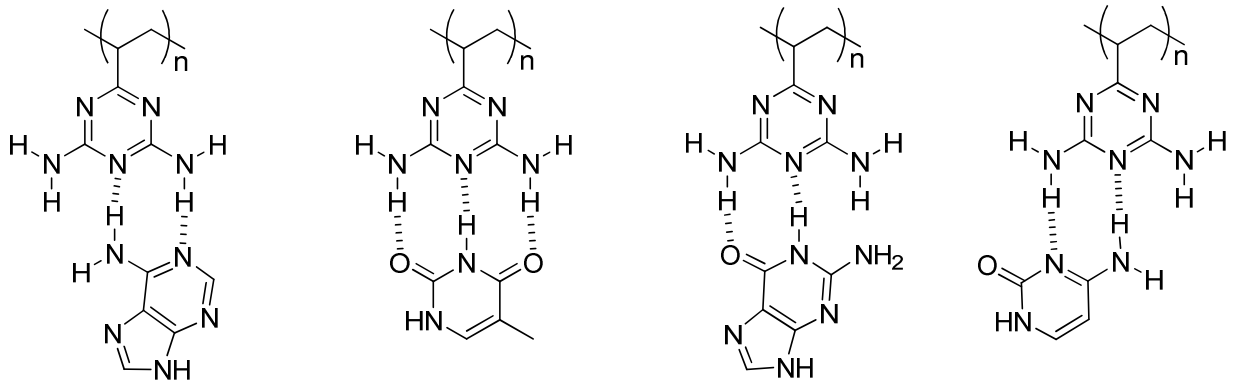

Figure 1.6. Hydrogen bonding interactions between nucleic acid bases and the DAT residue

Uracil, thymine, and guanine, show three hydrogen bonding sites toward PVDAT while adenine and cytosine show two hydrogen bonding sites (Fig. 1.6).[58,59] Differences in binding strengths can also be attributed to the neighboring group effect. The investigation of hydrogen bonding interactions was performed initially in water since the recognition of the various binding motifs that PDVAT demonstrates in water is critical for biological applications.[56] Water molecules show competitive binding of molecules though hydrogen bond interactions.[56] Comparison of binding efficiencies of PVDAT to nucleic acid bases in water and in methanol revealed greater binding strengths in water for the purine bases while pyrimidine bases showed little variability between the two solvents.[58] Discrepancies in the binding strengths of purine bases in water and methanol is attributed to both stacking and apolar interactions that occur in the water solution.[58]

The comparison of the binding abilities of PVDAT to nucleic acid bases and that of the corresponding monomers demonstrated the necessity of the polymeric structure for hydrogen bond formation.[57] It was proposed that PVDAT forms apolar microspheres at the sites where hydrogen bonding occurs, which encourages hydrogen-bond formation

between PVDAT and dsDNA over the formation of binding interactions with dsDNA and water molecules.[58] It was observed that nucleotides and dinucleotides had stronger binding interactions with PVDAT than nucleic acid bases indicating the importance of the electrostatic interactions between the negatively charged backbone of DNA and the protonated amine on cationic DAT residues.[57]

The ability to recognize A-T base pairs in the major groove of dsDNA was also investigated in the preparation of an imprinted polymer film containing PVDAT.[61] Detection of the binding interaction between VDAT and A-T base pairs, which is depicted in Fig. 1.7, was accomplished using NMR, which showed chemical shifts consistent with the expected hydrogen bonding interactions.[61] Melting point analysis of poly(dA)-poly(dT) dsDNA molecules showed an increase in the melting temperature of these model dsDNA molecules when in the presence of VDAT, which is attributed to hydrogen bonding interactions since electrostatic interactions were negligible at the solution pH.[61] CD spectral analysis was utilized to exclude the possibility of intercalation contributing to the binding of VDAT to poly(dA)-poly(dT) dsDNA molecules.[61] Fluorescence analysis allowed for comparison of the imprinted polymer film and the non-imprinted polymer film.[61] Detection of a distinct increase in fluorescence intensity for the imprinted polymer film as compared to the non-imprinted film suggested selective binding of DNA with the imprinted polymer.[61]

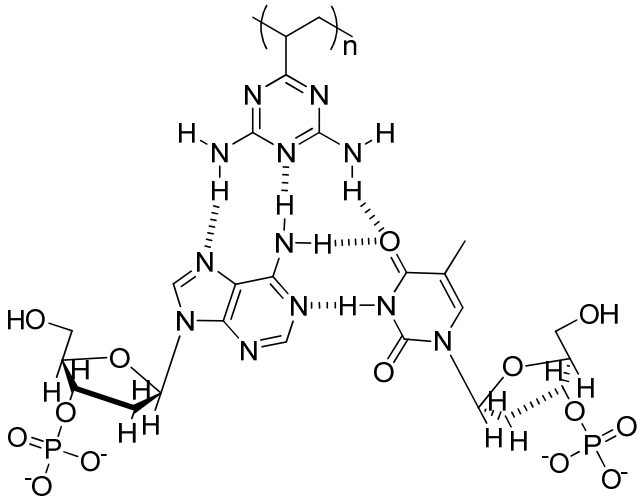

Figure 1.7. Proposed hydrogen bonding interactions between PVDAT and the A-T base pair

A non-electrostatic gene delivery system based on PVDAT and its copolymers with poly(1-vinyl-2-pyrrolidone) (VP) were investigated to evaluate transfection efficiencies with decreased or no electrostatic interactions and predominantly hydrogen bonding interactions.[14] Complexation of these polymers with pDNA showed increased retardation in the migration through electrophoresis gel with the addition of increasing weight ratios (PVDAT:pDNA) consistent with the electrophoresis migration model for non-electrostatic interactions between DNA and its binding agents as found with Hoechst 33258.[14,19] Transfection of luciferase-encoded pDNA to COS-1 cells was shown to have high efficiency as well as noticeably lower cytotoxicity with the VDAT based gene delivery vectors as compared to the widely studied ExGen 500 complexes.[14] Research into these hydrogen-bond interaction based vectors also showed decreased nuclease-mediated degradation of pDNA when bound with PVDAT. The stability of these complexes to that of ExGen 500 complexes in serum showed increased stability as compared to complexes with PVDAT.[14,19] Further investigation of PVDAT as a gene

delivery agent focused on the cellular internalization of these polyplexes.[48] Knockdown studies of the various endocytic pathways suggested that the polyplexes are internalized via a non-clathrin, non-caveolae mediated endocytosis.[48]

1.5 Effects of hydrogen bonding on gene delivery with poly(glycoamidoamine)s

Design of poly(glycoaminoamine) (PGAA) based gene delivery vectors was based on structural features of two previously investigated gene delivery agents.[69] These vectors are previously reported as having high transfection efficiencies due to the ability of protonated secondary amines in the polymer backbone to effectively condense DNA as well as undesirable high cytotoxic effects.[13,40,70-76] Chitosan, a polysaccharide, contains primary amines rather than secondary amines and shows effective binding and condensation of pDNA.[77-85] This gene delivery vector is reported to show only minimal cytotoxicity even at high concentrations; however it was demonstrated as yielding poor gene expression efficiencies.[69] PGAA gene delivery agents (Fig. 1.8) combine structural features of both of these previously investigated vectors with the incorporation of carbohydrate residues in a backbone that resembles PEI.[17,36,69,86,87] Gel electrophoresis of polyplexes formed between low molecular weight PGAAs and pDNA, show a correlation between the binding affinity of the polyplex and both key structural features of PGAAs, the carbohydrate and amine functional groups.[69] Further investigation into these polyplexes using dynamic light scattering suggested that the stereochemistry of both the hydroxyl groups of the carbohydrate and the amine groups impact the condensation of pDNA upon polyplex formation.[69] One notable trend observed for the polymer structures containing four amine groups and varying in the stereochemistry of the hydroxyl groups of the carbohydrate was that these structures showed the highest transfection

efficiencies.[69] One key issue with these delivery vectors is the typically low molecular weight due to the strong experimental correlation between an increase in the molecular weight of a polymer and improved transfection efficiencies.

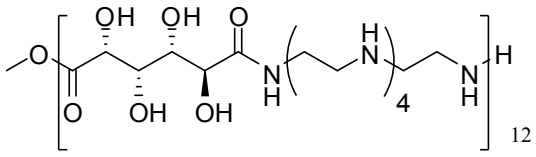

D4
Poly(D-glucaramidopentaethylenetrtramine)

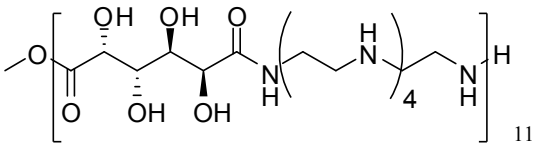

G4
Poly(galactaramidopentaethylenetrtramine)

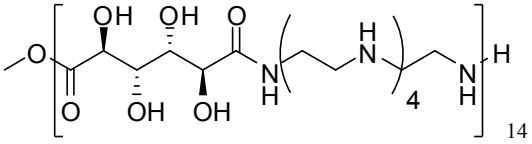

M4
Poly(D-mannaramidopentaethylenetrtramine)

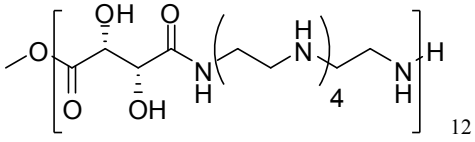

T4
Poly(L-tartaramidopentaethylenetrtramine)

Figure 1.8. PGAAs demonstrating the highest gene transfection efficiencies

Polyplex formation with PGAAs was also shown to result in the prevention of nuclease-mediated degradation of the pDNA using gel electrophoresis studies.[17] Comparison of the four polymer compositions exhibiting the highest gene transfection efficiencies showed that G4 and T4 were better able to protect pDNA from degradation.[17] The decreased ability to protect pDNA from degradation observed for D4 and M4 is attributed to the weaker binding affinities previously mentioned for these complexes.[17] The T4 structure demonstrated the highest polyplex stability and bond strengths however were not shown to give increased cellular uptake or gene expression, suggesting that the

polymer structure also greatly influences the transfection efficiency.[17] This trend prompted further investigation into the binding mechanism of these vectors with pDNA.[87]

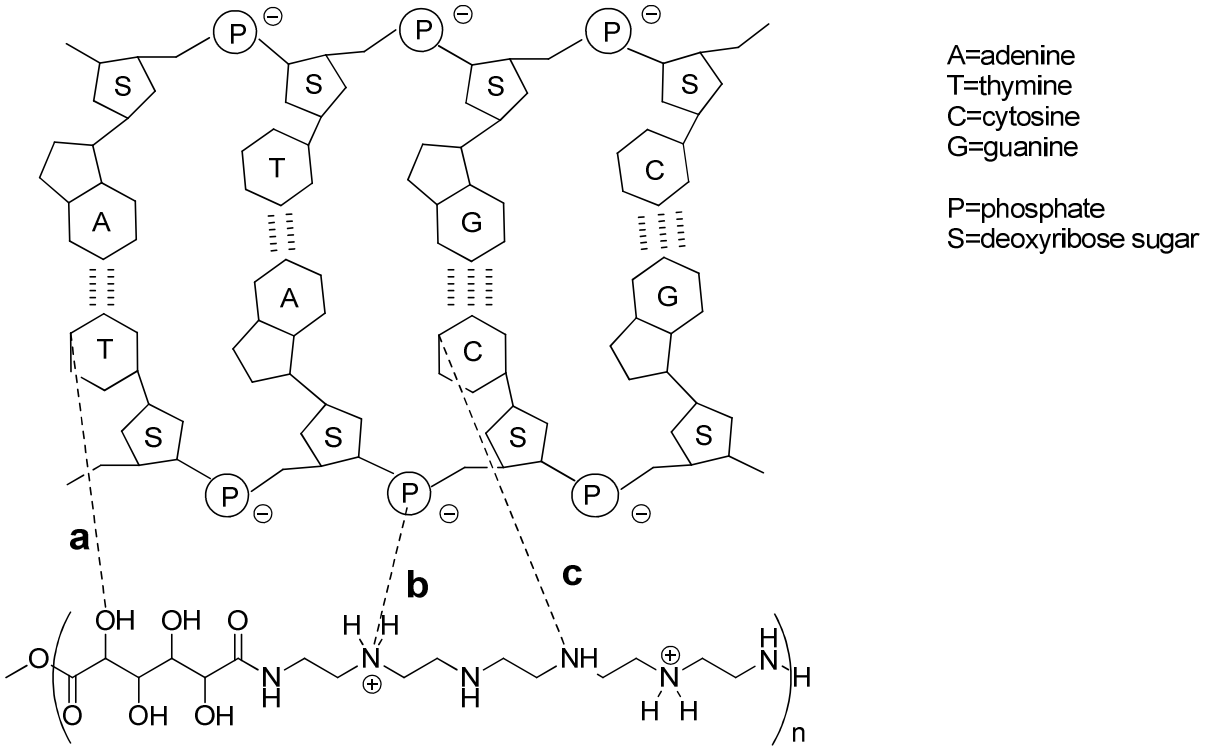

Figure 1.9. Binding of pDNA to PGAA via electrostatic interactions and hydrogen bonding interactions: (a) hydrogen bond interaction between a polymer hydroxyl functional group and a nucleic acid base, (b) electrostatic interactions between a protonated amine and the negatively charged phosphate group in the DNA backbone, and (c) hydrogen bonding interaction between a polymer amine functional group and a nucleic acid base[87]

A detailed study of the role of hydrogen bonding interactions in polyplex formation with pDNA and PGAA vectors was conducted comparing PGAAs shown to have the highest transfection efficiencies.[87] Expected mechanisms of polyplex formation include electrostatic interactions, hydrogen bonding interactions as depicted in Figure 1.9, as well as hydrophobicity.[87] Hydrophobic interactions were shown to play an inconsequential role in the formation of the polyplexes; however differences in the free binding energies when the only structural variation is the quantity and stereochemistry of

hydroxyl functional groups from the carbohydrate group suggests the significance of hydrogen bonding interactions in the binding affinities of these polymers structures.[87] Isothermal titration calorimetry assays in various buffers allowed for deconvolution of the free binding energies from electrostatic interactions, providing further evidence for the importance of hydrogen bonding interactions in these complexes.[87] Circular dichroism analysis of the complexes suggested specific hydrogen bonding motifs with pDNA, which lies in accordance with the dependence of binding affinities on the stereochemistry of the hydroxyl functional groups.[87] Determination of the binding mechanism between pDNA and the PGAA gene delivery agents provides a great deal of information concerning the structure-property relationships of these vectors, specifically concerning the importance of the hydrogen bonding interactions.[87]

1.5 Conclusions

The design of gene delivery agents based on non-electrostatic interactions, specifically hydrogen bonding interactions, were recently investigated towards optimization of polyplex formation resulting in efficient gene expression. Research into the relationship of hydrogen bonding groups and the subsequent increase in transfection efficiencies was reported for vectors incorporating small molecule Hoechst 33258, which is known to effectively bind the minor groove of dsDNA, into polyplexes previously shown to possess high transfection capabilities as well as high cytotoxicity. The study reported increase transfection efficiencies after incorporation of the hydrogen-bonding group, suggesting the role of these small molecules in the increased cellular uptake as well as producing variations in the intracellular trafficking of the polyplexes.

Incorporation of the hydrogen-bonding group into the polymeric structure was achieved in the design of PDVAT based gene delivery vectors. Intracellular routing of these polyplexes showed variation in the endocytic route as compared to that on PDMAEMA, suggesting the pivotal role cellular uptake mechanisms play in gene expression as well as the dependence of intracellular trafficking mechanisms on the interactions observed between polymer and DNA. The importance of hydrogen bonding interactions was also confirmed in vectors based on PGAAs, which showed both electrostatic and non-electrostatic interactions upon formation of the polyplex. These results suggest that incorporation of strong hydrogen bonding motifs into the polymeric structure could reduce or eliminate the necessity of the cationic character of previously investigated non-viral gene delivery agents, which is hypothesized to significantly decrease the cytotoxicity observed in current cationic polyelectrolyte vectors.

1.7 References

(1) Goldspiel, B. R.; Green, L.; Calis, K. A. *Clinical Pharmacy* **1993**, *12*, 488.
(2) Hallez, S. *Revue Des Maladies Respiratoires* **1995**, *12*, 567.
(3) Niazi, G. A. *Saudi Medical Journal* **1997**, *18*, 1.
(4) Pappas, M. G. *Drug Development and Industrial Pharmacy* **1996**, *22*, 791.
(5) Sandhu, J. S.; Keating, A.; Hozumi, N. *Critical Reviews in Biotechnology* **1997**, *17*, 307.
(6) Savill, J. *British Medical Journal* **1997**, *314*, 126.
(7) Valere, T. *M S-Medecine Sciences* **1996**, *12*, 73.
(8) Yanez, R. J.; Porter, A. C. G. *Gene Therapy* **1998**, *5*, 149.
(9) Davis, M. E. *Curr. Opin. Biotechnol.* **2002**, *13*, 128.
(10) Kodama, K.; Katayama, Y.; Shoji, Y.; Nakashima, H. *Current Medicinal Chemistry* **2006**, *13*, 2155.
(11) Pack, D. W.; Hoffman, A. S.; Pun, S.; Stayton, P. S. *Nat. Rev. Drug Discov.* **2005**, *4*, 581.
(12) Tiera, M. J.; Winnik, F. M.; Fernandes, J. C. *Curr. Gene Ther.* **2006**, *6*, 59.
(13) Boussif, O.; Lezoualch, F.; Zanta, M. A.; Mergny, M. D.; Scherman, D.; Demeneix, B.; Behr, J. P. *Proceedings of the National Academy of Sciences of the United States of America* **1995**, *92*, 7297.
(14) Cao, Z. Q.; Liu, W. G.; Liang, D. C.; Guo, G.; Zhang, J. Y. *Advanced Functional Materials* **2007**, *17*, 246.
(15) Fong, S.; Liu, Y.; Heath, T.; Fong, P.; Liggitt, D.; Debs, R. J. *Molecular Therapy* **2004**, *10*, 706.
(16) Heath, W. H.; Senyurt, A. F.; Layman, J.; Long, T. E. *Macromolecular Chemistry and Physics* **2007**, *208*, 1243.
(17) Liu, Y. M.; Reineke, T. M. *Bioconjugate Chemistry* **2006**, *17*, 101.
(18) Pouton, C. W.; Seymour, L. W. *Advanced Drug Delivery Reviews* **2001**, *46*, 187.
(19) Soto, J.; Bessodes, M.; Pitard, B.; Mailhe, P.; Scherman, D.; Byk, G. *Bioorganic & Medicinal Chemistry Letters* **2000**, *10*, 911.
(20) van der Aa, M. A. E. M.; Huth, U. S.; Hafele, S. Y.; Schubert, R.; Oosting, R. S.; Mastrobattista, E.; Hennink, W. E.; Peschka-Suss, R.; Koning, G. A.; Crommelin, D. J. A. *Pharmaceutical Research* **2007**, *24*, 1590.
(21) Arigita, C.; Zuidam, N. J.; Crommelin, D. J. A.; Hennink, W. E. *Pharmaceutical Research* **1999**, *16*, 1534.
(22) Dubruel, P.; Schacht, E. *Macromolecular Bioscience* **2006**, *6*, 789.
(23) Jeong, J. H.; Kim, S. W.; Park, T. G. *Progress in Polymer Science* **2007**, *32*, 1239.
(24) Lee, J. H.; Ahn, H. H.; Shin, Y. N.; Kim, M. S.; Hwang, K. C.; Lee, B.; Khang, G.; Lee, H. B. *Tissue Engineering and Regenerative Medicine* **2007**, *4*, 341.
(25) Verbaan, F. J.; Bos, G. W.; Oussoren, C.; Woodle, M. C.; Hennink, W. E.; Storm, G. *Journal of Drug Delivery Science and Technology* **2004**, *14*, 105.
(26) Volcke, C.; Pirotton, S.; Grandfils, C.; Humbert, C.; Thiry, P. A.; Ydens, I.; Dubois, P.; Raes, M. *Journal of Biotechnology* **2006**, *125*, 11.
(27) Agarwal, A.; Mallapragada, S. K. *Current Topics in Medicinal Chemistry* **2008**, *8*, 311.

(28) Green, J. J.; Langer, R.; Anderson, D. G. *Accounts of Chemical Research* **2008**, *41*, 749.
(29) Hou, S.; Yang, K.; Yao, Y.; Liu, Z.; Feng, X. Z.; Wang, R.; Yang, Y. L.; Wang, C. *Colloids and Surfaces B-Biointerfaces* **2008**, *62*, 151.
(30) Ji, W. H.; Lin, L.; Chen, D. Y.; Liu, W. G. *Progress in Chemistry* **2008**, *20*, 936.
(31) Jiang, X.; Lok, M. C.; Hennink, W. E. *Bioconjugate Chemistry* **2007**, *18*, 2077.
(32) Kasyanenko, N.; Afanasieva, D.; Dribinsky, B.; Mukhin, D.; Nazarova, O.; Panarin, E. *Structural Chemistry* **2007**, *18*, 519.
(33) Ko, I. K.; Ziady, A.; Lu, S. W.; Kwon, Y. J. *Biomaterials* **2008**, *29*, 3872.
(34) Kreppel, F.; Kochanek, S. *Molecular Therapy* **2008**, *16*, 16.
(35) Lavigne, M. D.; Pennadam, S. S.; Ellis, J.; Alexander, C.; Gorecki, D. C. *Journal of Gene Medicine* **2007**, *9*, 44.
(36) Lee, C. C.; Liu, Y.; Reineke, T. M. *Bioconjugate Chemistry* **2008**, *19*, 428.
(37) Lin, S.; Du, F. S.; Wang, Y.; Ji, S. P.; Liang, D. H.; Yu, L.; Li, Z. C. *Biomacromolecules* **2008**, *9*, 109.
(38) Piest, M.; Lin, C.; Mateos-Timoneda, M. A.; Lok, M. C.; Hennink, W. E.; Feijen, J.; Engbersen, J. F. J. *Journal of Controlled Release* **2008**, *130*, 38.
(39) Slita, A. V.; Kasyanenko, N. A.; Nazarova, O. V.; Gavrilova, II; Eropkina, E. M.; Sirotkin, A. K.; Smirnova, T. D.; Kiselev, O. I.; Panarin, E. F. *Journal of Biotechnology* **2007**, *127*, 679.
(40) Turk, M.; Dincer, S.; Piskin, E. *Journal of Tissue Engineering and Regenerative Medicine* **2007**, *1*, 377.
(41) Wang, C.; Pham, P. T. *Expert Opinion on Drug Delivery* **2008**, *5*, 385.
(42) Wong, S. Y.; Pelet, J. M.; Putnam, D. *Progress in Polymer Science* **2007**, *32*, 799.
(43) You, Y. Z.; Manickam, D. S.; Zhou, Q. H.; Oupicky, D. In *13th International Symposium on Recent Advances in Drug Delivery*; Elsevier Science Bv: Salt Lake City, UT, 2007, p 217.
(44) Khalil, I. A.; Kogure, K.; Akita, H.; Harashima, H. *Pharmacological Reviews* **2006**, *58*, 32.
(45) Anderson, R. G. W. *Annual Review of Biochemistry* **1998**, *67*, 199.
(46) Rejman, J.; Bragonzi, A.; Conese, M. *Molecular Therapy* **2005**, *12*, 468.
(47) Lechardeur, D.; Verkman, A. S.; Lukacs, G. L. *Adv. Drug Deliv. Rev.* **2005**, *57*, 755.
(48) Ye, G. X.; Cao, Z. Q.; Lin, L.; Chen, D. Y.; Liu, W. G. *Chinese Science Bulletin* **2008**, *53*, 2307.
(49) vandeWetering, P.; Cherng, J. Y.; Talsma, H.; Hennink, W. E. *Journal of Controlled Release* **1997**, *49*, 59.
(50) Layman, J. M.; Ramirez, S. M.; Green, M. D.; Long, T. E. *Biomacromolecules* **2009**, *10*, 1244.
(51) Neidle, S. *Natural Product Reports* **2001**, *18*, 291.
(52) Sponer, J.; Leszczynski, J.; Hobza, P. *Journal of Biomolecular Structure & Dynamics* **1996**, *14*, 117.
(53) Buurma, N. J.; Haq, I. *Journal of Molecular Biology* **2008**, *381*, 607.
(54) Loontiens, F. G.; Regenfuss, P.; Zechel, A.; Dumortier, L.; Clegg, R. M. *Biochemistry* **1990**, *29*, 9029.

(55) Guan, Y.; Shi, R.; Li, X. M.; Zhao, M. P.; Li, Y. Z. *Journal of Physical Chemistry B* **2007**, *111*, 7336.
(56) Asanuma, H.; Ban, T.; Gotoh, S.; Hishiya, T.; Komiyama, M. *Macromolecules* **1998**, *31*, 371.
(57) Asanuma, H.; Ban, T. S.; Gotoh, S.; Hishiya, T.; Komiyama, R. *Supramol. Sci.* **1998**, *5*, 405.
(58) Asanuma, H.; Hishiya, T.; Ban, T.; Gotoh, S.; Komiyama, M. *J. Chem. Soc.-Perkin Trans. 2* **1998**, 1915.
(59) Ma, H. M.; Nie, L. H.; Xiong, S. X. *Supramol. Chem.* **2004**, *16*, 311.
(60) Nie, L. H.; Ma, H. M.; Li, X. H.; Sun, M.; Xiong, S. X. *Biopolymers* **2003**, *72*, 274.
(61) Slinchenko, O.; Rachkov, A.; Miyachi, H.; Ogiso, M.; Minoura, N. *Biosens. Bioelectron.* **2004**, *20*, 1091.
(62) Binder, W. H.; Zirbs, R. In *Hydrogen Bonded Polymers*; Springer-Verlag Berlin: Berlin, 2007; Vol. 207, p 1.
(63) Jorgensen, W. L.; Pranata, J. *Journal of the American Chemical Society* **1990**, *112*, 2008.
(64) Lawrence, D. S.; Jiang, T.; Levett, M. *Chemical Reviews* **1995**, *95*, 2229.
(65) Lehn, J. M. In *4th European Polymer Federation Symp on Polymeric Materials*; Huthig & Wepf Verlag: Baden Baden, Germany, 1992, p 1.
(66) Lehn, J. M. In *Conference on the Nato Advanced Research Workshop on Supramolecular Science - Where It is and Where It is Going*; Ungaro, R. D. E., Ed.; Springer: Lerici, Italy, 1998, p 287.
(67) Reinhoudt, D. N.; Stoddart, J. F.; Ungaro, R. *Chemistry-a European Journal* **1998**, *4*, 1349.
(68) Krische, M. J.; Lehn, J. M. In *Molecular Self-Assembly* 2000; Vol. 96, p 3.
(69) Liu, Y. M.; Reineke, T. M. *Journal of the American Chemical Society* **2005**, *127*, 3004.
(70) Densmore, C. L. *Expert Opinion on Biological Therapy* **2003**, *3*, 1083.
(71) Ito, T.; Iida-Tanaka, N.; Koyama, Y. *Journal of Drug Targeting* **2008**, *16*, 276.
(72) Kakimoto, S.; Moriyama, T.; Tanabe, T.; Shinkai, S.; Nagasaki, T. *Journal of Controlled Release* **2007**, *120*, 242.
(73) Lee, J. H.; Ahn, H. H.; Shin, Y. N.; Kim, M. S.; Lee, B.; Khang, G.; Lee, I.; Lee, H. B. *Tissue Engineering and Regenerative Medicine* **2007**, *4*, 566.
(74) Paris, S.; Burlacu, A.; Durocher, Y. *Journal of Biological Chemistry* **2008**, *283*, 7697.
(75) Sakae, M.; Ito, T.; Yoshihara, C.; Iida-Tanaka, N.; Yanagie, H.; Eriguchi, M.; Koyama, Y. *Biomedicine & Pharmacotherapy* **2008**, *62*, 448.
(76) Sundaram, S.; Lee, L. K.; Roth, C. M. *Nucleic Acids Research* **2007**, *35*, 4396.
(77) Behr, J. P. *Bioconjugate Chemistry* **1994**, *5*, 382.
(78) Bowman, K.; Leong, K. W. *International Journal of Nanomedicine* **2006**, *1*, 117.
(79) Hein, S.; Wang, K.; Stevens, W. F.; Kjems, J. *Materials Science and Technology* **2008**, *24*, 1053.
(80) Jiang, H. L.; Arote, R.; Jere, D.; Kim, Y. K.; Cho, M. H.; Cho, C. S. *Materials Science and Technology* **2008**, *24*, 1118.

(81) Kudsiova, L.; Arafiena, C.; Lawrence, M. J. *Journal of Pharmaceutical Sciences* **2008**, *97*, 3981.
(82) Lee, K. Y. *Macromolecular Research* **2007**, *15*, 195.
(83) Prabaharan, M. *Journal of Biomaterials Applications* **2008**, *23*, 5.
(84) Prabaharan, M.; Mano, J. F. *Drug Delivery* **2005**, *12*, 41.
(85) Ghosn, B.; Kasturi, S. P.; Roy, K. *Current Topics in Medicinal Chemistry* **2008**, *8*, 331.
(86) Liu, Y. M.; Wenning, L.; Lynch, M.; Reineke, T. M. *Journal of the American Chemical Society* **2004**, *126*, 7422.
(87) Prevette, L. E.; Kodger, T. E.; Reineke, T. M.; Lynch, M. L. *Langmuir* **2007**, *23*, 9773.

Chapter 2. Structure-Property Relationships of Adenine- and Thymine-Containing Poly(2-(dimethylamino) ethyl methacryate)

2.1 Abstract

Polymer containing electrostatic interactions and polymers containing hydrogen bonding motifs are both extensively discussed in literature, however the combination of electrostatic and hydrogen bonding interactions is not widely investigated in current literature. A series of adenine- and thymine-containing PDMAEMA copolymers were synthesized to investigate the effect of incorporating hydrogen bonding groups into a polyelectrolyte. Polyelectrolytes containing hydrogen bonding groups are expected to exhibit properties of both classes of supramolecular interactions. *In situ* FTIR analysis of the polymerization reveals the reaction reaches completion after 24 hours and allowed for analysis of the reaction kinetics as well as determination of the reactivity ratios using the Mayo-Lewis determination method. TGA and DSC were utilized in the characterization of the thermal properties of the nucleobase-containing PDMAEMA copolymers. Incorporation of the styrenic nucleobases significantly affected the solubility of the copolymers and prevented molecular weight analysis using SEC. Incorporation of the nucleobases also significantly affected the solubility of these copolymers on aqueous solutions and showed salt-triggerability with higher contents of these groups. Solution rheology also revealed the influence of hydrogen bonding on the apparent viscosity and entanglement concentrations of these polyelectrolytes.

2.2 Introduction

Supramolecular chemistry refers to the area of chemistry that focuses on the polymeric polymers composed of a self-assembled molecular subunits or components.[1-9] Supramolecular self-assembly occurs through a number of noncovalent interactions including hydrogen bonding, metal coordination, hydrophobic interactions, and electrostatic effects.[1] A large percent of current research efforts focus on self-assembly through various hydrogen bonding arrays, including those observed for nucleic acid base pairs..[1-5,10-12] Self-assembly of two strands of DNA with complementary nucleic acid sequences, a naturally occurring supramolecular complex, shows high specificity due to the complementary hydrogen bonding arrays of the various nucleobases.[1]

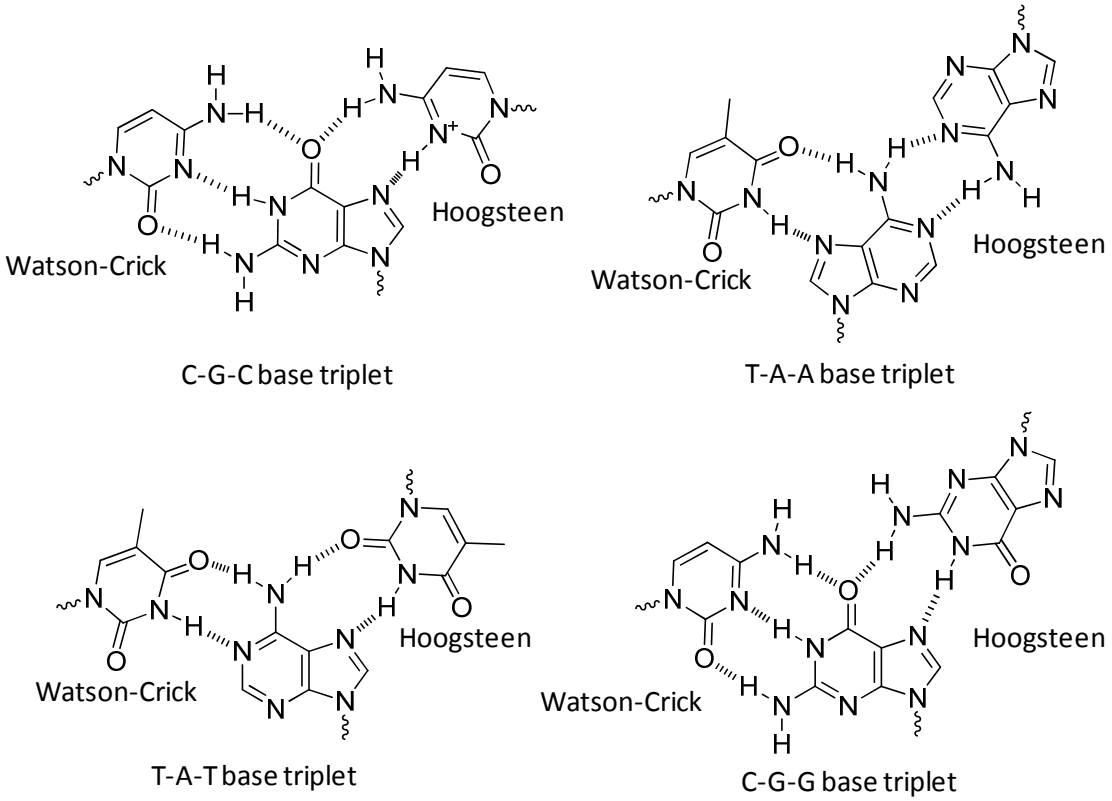

Figure 2.1. Watson-Crick and Hoogsteen Base Pair Interactions[13]

The hydrogen bonding motifs between the complementary nucleic acid base pairs, known as Watson-Crick base pairs, form the basis of the double helix structure observed in double stranded DNA.[13,14] While bound to the double helix structure of dsDNA these base pairs demonstrate the ability to act as both hydrogen bond donors and acceptors.[14] Hoogsteen base pair interactions, depicted in conjunction with Watson-Crick base-pairs in Figure 1, allow for triplex DNA formation in the DNA minor groove.[15]

Supramolecular complexes based on nucleobases show high specificity due to the highly conserved hydrogen bonding interactions between the complementary nucleobases.[1] The predictability of interactions between long sequences of nucleic acids makes the utilization of nucleobases for hydrogen binding motifs desirable.[16] This allows great flexibility for the formation of hydrogen bonds between the polymer chains. Supramolecular complexation between nucleobase-functionalized compounds significantly alters the properties of these materials. The well-defined hydrogen bonding interactions between the nucleobases provide the thermodynamic stability required for the self-assembly of these structures. Side-chain functionalized polymers demonstrate the capability of DNA-like assembly of the polymer chains. Complexation of side-chain functionalized polymers and nucleobase-functionalized monomers significantly alters the bulk state properties of the polymer.

Placement of nucleobases on polymer side-chains provides another method for incorporating nucleobases into polymers, which is achieved with nucleobase-substitution of polymerizable groups such as styrene (Figure 2.2).[17-20]

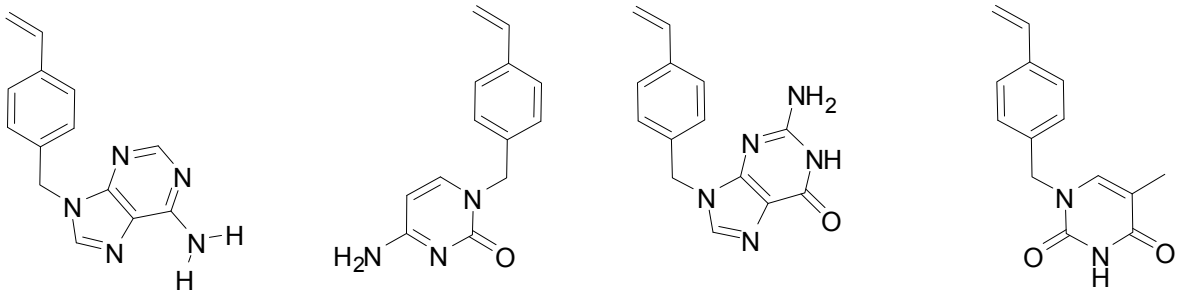

Figure 2.2. 4-(vinyl benzyl) derivatives of (1) adenine, (2) guanine, (3) cytosine, and (4) thymine[17-20]

Research efforts of Long and coworkers include synthesis of nucleobase-containing triblock copolymers by nitroxide mediated polymerization (NMP), a controlled radical polymerization method enabling block copolymer synthesis with a wide range of acrylic and styrenic monomers.[11] The stoichiometric ratio between nucleobase-functionalized monomer units and the co-monomer units in the polymer chain remains the key factor influencing self-assembly of the copolymers in a noncompetitive solvent as seen in the research efforts of Lutz and coworkers.[10] Solvents such as water competitively form hydrogen bonding interactions with the nucleobases on the polymer, disrupting the interactions between the polymer chains. This prevents accurate analysis of the strength of the hydrogen bonding interactions between the polymer chains. Both the adenine-functionalized and thymine-functionalized copolymers form spherical colloids in noncompetitive solvents. Colloid rearrangement occurs upon mixing of the two nucleobase-functionalized copolymer solutions since thermodynamics favor the adenine-thymine interactions over thymine-thymine or adenine-adenine interactions. The resulting dispersions become more thermally stable than the original solutions containing only the thymine-functionalized copolymer of the adenine-functionalized copolymer. All of the supramolecular complexes show stability in solution over long periods, and easily

break apart and reform with changes in temperature due the dissociation and association of intermolecular hydrogen bonds.[21] The addition of the nucleobase-functionalized monomers to the copolymer solutions results in the formation of smaller aggregates; this suggests the dissociation of polymer-polymer complexes and the association of monomer-polymer complexes.[21]

Comparison of the affinity of homopolymers of each of the nucleobase-containing monomers for dsDNA allows for investigation into the binding affinities of these nucleobase-containing monomers for nucleic acid base pairs. Predicted variations in binding affinities will result from the variation in the binding affinities exhibited in each of the nucleic acid bases.[4,22-26] Free-radical polymerization of the nucleobase-functionalized monomers 9-(4-vinylbenzyl) adenine (VBA) and 1-(4-vinylbenzyl) thymine (VBT) yield materials exhibiting self-recognition abilities similar to complementary DNA molecules.[10,21,27] Cooperative intermolecular hydrogen bonding make PVBA and PVBT homopolymers insoluble in most organic solvents and therefore impractical for most applications.[10,21] The physical gel that are characteristic of this class of polymer is disrupted with competitive solvents such as dimethyl sulfoxide (DMSO), which binds with the hydrogen bonding motifs of the nucleobases and prevents self-association.[10]

Copolymerization of the nucleobase-containing monomers with a monomer such as dodecyl methacrylate allows for the modification of the polymer solubility.[10,21,27] The long alkyl chains on this co-monomer increase the solubility of the copolymers in noncompetitive solvents, enabling the investigation into self-assembly processes.[10,21] The adenine- and thymine-functionalized copolymers self-assemble based on the

complementary hydrogen bonding arrays of these nucleobases. [27] The supramolecular complexes show temperature dependant changes in intensity for the IR and UV-vis absorption spectra, indicating "melting" behavior similar to the double strand to single strand transition observed for DNA.[27]

Electrostatic interactions are also a mode of supramolecular self-assembly. Polyelectrolytes are a class of polymers that contain a high concentration of repeating units containing ionizable groups which, when in solution, is balanced with a cloud of counterions.[28-30] The electrostatic interactions between these charged groups significantly influence the behavior of these polymers in aqueous solvents. Solution pH and temperature, strength of the ionic interactions and concentration also influence the behavior of polyelectrolytes. The combination of the electrostatic interactions of a polyelectrolyte with a repeating unit containing self-complementary hydrogen bonding interactions is expected to result in materials exhibiting interesting self-association based behavior resulting from both classes of intermolecular interactions.[31]

2.3 Experimental

2.3.1 Materials.

Adenine (99%) was purchased from Aldrich and 4-vinylbenzyl chloride (90%) purchased from Fluka, both were used as obtained. Potassium carbonate (99%) was purchased from Aldrich as used as obtained. Methanol (99.9%), dimethyl sulfoxide (99.9%), chloroform (99.9%) were purchased from Fisher as used as obtained. 2-(*N*,*N*′-Dimethylamino)ethyl methacrylate (DMAEMA, 99.5%, Fisher) was passed through a neutral alumina column

to remove free radical inhibitor. 2,2′-Azobisisobutyronitrile (AIBN, 99%, Sigma-Aldrich) was used as received. Deuterium oxide (D2O, 99.9%, Cambridge Isotope Laboratories) was used as received for all NMR measurements. Ultrapure water was obtained with a Millipore Direct-Q5 purification polymer. All other solvents were used as received from commercial sources without further purification.

2.3.2 Instrumentation.

^{1}H NMR spectroscopic data was collected in DMF-d_7, DMSO-d_6, and D_2O on a Varian 400 MHz spectrometer. Differential Scanning Calorimetry (DSC) was obtained with TA DSC Instruments under nitrogen at a heating and cooling rate of 10 ºC/min. Values from the second heating were reported. Thermogravimetric analysis (TGA) was performed on a TA Instruments TGA under a nitrogen atmosphere at a heating rate of 10 °C/min. *In situ* FTIR analysis was performed with a Metler Toledo ReactIR 45m instrument fitted with a di-comp fiber optic ATR probe. An average absorbance was plotted every 2 minutes from 256 infrared scans for 24 h. Dynamic light scattering (DLS) measurements were performed on a Malvern Zeta Sizer Nano Series Nano-ZS instrument using Dispersion Technology Software (DTS) version 4.20 at awavelength of 633 nm using a 4.0 mW, solid state He-Ne laser at a scattering angle of 173°. The experiments were performed in triplicate at a temperature of 25 °C.

2.3.3 Synthesis of 9-(4-Vinylbenzyl) Adenine.

A previously reported synthetic scheme was followed for the synthesis of 9-(4-vinylbenzyl) adenine.[19] A 250-mL round-bottomed flask was charged with adenine

(10.00 g, 74 mmol), 4-vinylbenzyl chloride (11.41 g, 74.74 mmol), tetramethyl ammonium iodide (44.6 mg, 0.22 mmol), potassium carbonate (13.70 g, 99.16 mmol), and anhydrous DMSO (100 mL). Nitrogen gas was bubbled through the reaction solution for approximately 30 min. The reaction solution was stirred at room temperature for 48 h. The solution was filtered and precipitated into distilled water. The product was recrystallized from a 1:3 chloroform:methanol solution four times and a white solid was obtained with 34% yield.

2.3.4 Synthesis of Poly(9-VBA-co-DMAEMA).

A 50-mL round-bottomed flask was charged with 9-(4-vinylbenzyl) adenine and *2*-(dimethylamino*)*ethyl methacrylate in varying amounts. The glassware was purged with nitrogen. Anhydrous DMF was added to make a 20 wt% solution. AIBN initiator (0.5 mol%) solution in anhydrous DMF was syringed into the reaction solution. The flask was immersed in an oil bath at 65 ^{o}C and stirred for 24 h at this temperature. The reaction solution was cooled to room temperature and diluted with an equal volume of chloroform. The resulting solution was precipitated into hexanes. The product was dried and then protonated by the addition of a 0.5 M HCl solution, which was allowed to stir for 6 h. The solution was precipitated into THF and dried overnight at 100 ^{o}C under vacuum.

2.3.5 Synthesis of 1-(4-Vinylbenzyl) Thymine.

A previously reported synthetic scheme was followed for the synthesis of 1-(4-vinylbenzyl)thymine.[19] Thymine (2.50g; 20 mmol) was dissolved in

hexamethyldisilazane (13 mL). The resulting solution was treated with trimethylsilyl chloride (1 mL) and refluxed under inert atmosphere for 24 h. The residual hexamethyldisilazane was removed by vacuum distillation. The silylated thymine was dissolved in DMF (10 mL). To the reaction flask was added 4-vinylbenzyl chloriode (3 mL, 21 mmol), NaI (30 mg, 0.2 mmol), and hydroquinone (10 mg). The mixture was stirred at 80 ^{o}C for 8 h. The mixture was then added dropwise to water (150 mL) and recrystallized three times from methanol to give 3.2 g (60%) of white crystals with a melting point of 164 ^{o}C as determined by DSC.

2.3.6 Synthesis of Poly(1-VBT-co-DMAEMA).

A 50-mL round-bottomed flask was charged with 1-(4-vinylbenzyl) thymine and 2-*(*dimethylamino*)*ethyl methacrylate in varying amounts. The glassware was purged with nitrogen. Anhydrous DMF was added to make a 20 wt% solution. AIBN initiator (0.5 mol%) solution in anhydrous DMF was syringed into the reaction solution. The flask was immersed in an oil bath at 65 ^{o}C and stirred for 24 h at this temperature. The reaction solution was cooled to room temperature and diluted with an equal volume of chloroform. The resulting solution was precipitated into hexanes. The product was dried and then protonated by the addition of a 0.5 M HCl solution, which was allowed to stir for 6 h. The solution was precipitated into THF and dried overnight at 100 ^{o}C under vacuum.

2.4 Results and Discussion

2.4.1 Synthesis and characterization of nucleobase-containing Poly(N,N-dimethylamino ethyl methacrylate)

The goal was to synthesize a series of nucleobase-containing polyelectrolytes containing various amounts of the hydrogen bonding groups in order to investigate the effect of the incorporation of hydrogen bonding on thermal, mechanical, and biological properties of polyelectrolytes. Schemes for the synthesis of the nucleobase-containing monomers depicted in Figure 2.3 and 2.4 include the covalent attachment of each nucleobase to a styrene. Preparation of vinyl-substituted nucleobases provides one method of incorporating nucleobase groups in a polymeric structure. Consistency in the linker unit allows for a more accurate comparison of the structure-property relationships observed upon incorporation of each nucleobase-containing monomer.

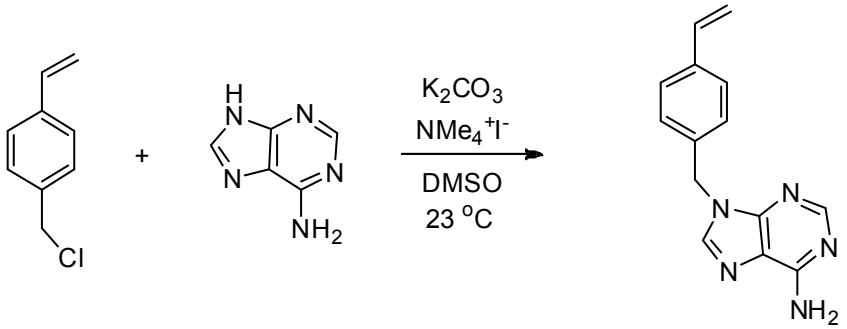

Figure 2.3. Synthesis of 9-(4-vinylbenzyl) adenine (9-VBA)

Protection of the carbonyl groups prior to styrene functionalization in the synthesis of 1-VBT (Figure 2.4) is necessary to insure the hydrogen-bonding sites remain unreacted and therefore able to participate in complex formation one included in the polymer structure.

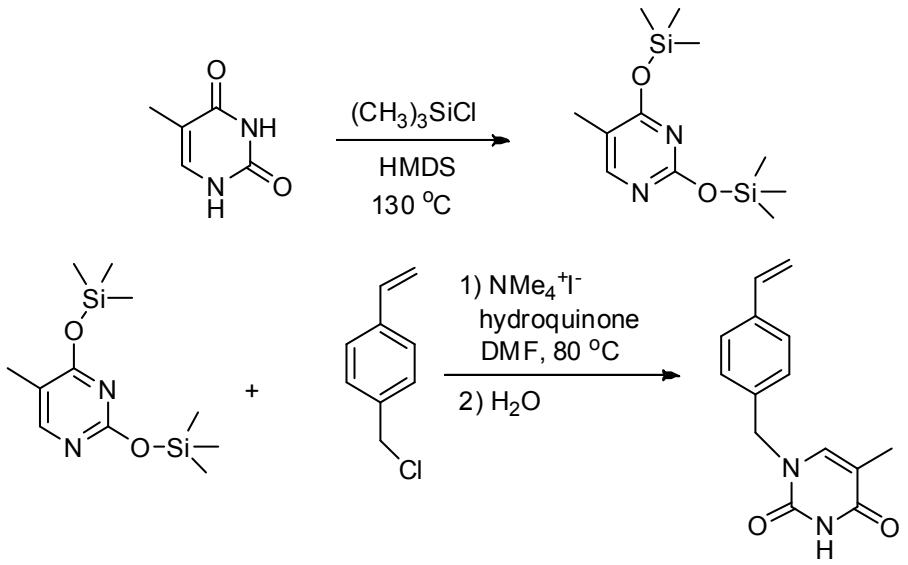

Figure 2.4. Synthesis of 1-(4-vinylbenzyl) thymine

The synthesis of nucleobase-containing copolymers was performed in DMF due to the insolubility of the nucleobase-functionalized monomers in most common solvents (Figure 2.5). Prior to addition of DMAEMA and AIBN to the reaction flask, the styrenic monomers were heated in DMF while stirring to ensure the solution was homogenous prior to initiating polymerization. Once heated the reaction solutions remained homogenous for the duration of the polymerization. *In situ* FTIR spectroscopy was utilized in monitoring the polymerizations ensuring the polymerization reactions went to completion and to determine the degree of polymerization, which was determined as 60% for these reactions. The reaction kinetics for the polymerization of 9-VBA and DMAEMA are further discussed in section 2.4.3.

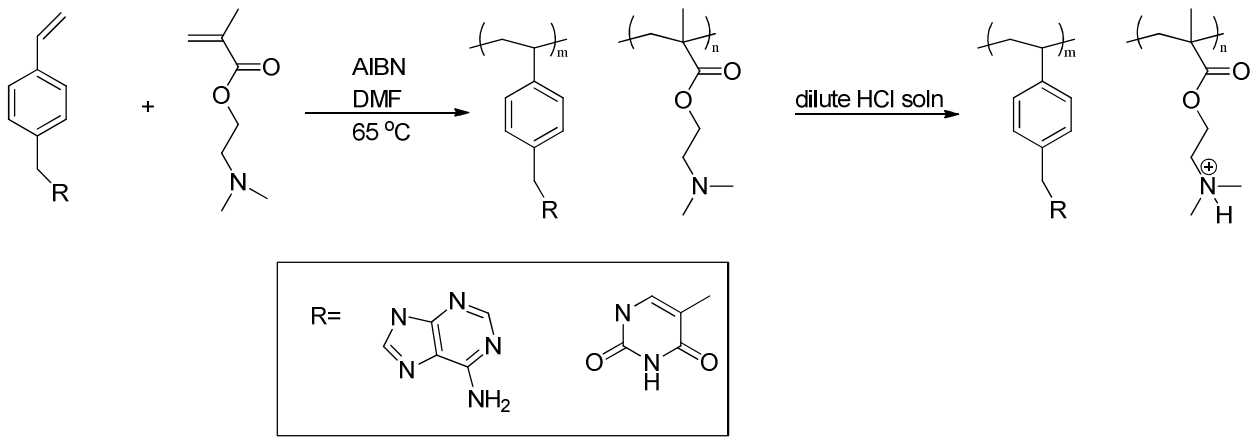

Figure 2.5. Synthesis of nucleobase-containing PDMAEMA

The chemical structure of the protonated copolymers was confirmed using ^{1}H NMR spectroscopy. Molecular weight analysis was not able to be performed using size-exclusion chromatography (SEC) in organic solvents due to insolubility (THF and chloroform) or aggregation (DMF and DMF/LiBr) of the dried polymer samples. The insolubility is mainly attributed to the insolubility of the styrenic nucleobase monomers since the homopolymer PDMAEMA is soluble in many common SEC solvents. Aggregation of the copolymers in DMF is also attributed to the nucleobase groups due to the high association constant for the hydrogen bonding interactions between nucleobases. SEC analysis on aggregated polymers leads to inaccurate measurements of molecular weight; therefore solution must be shown to allow for free random polymer coils. Dynamic light scattering (DLS) was utilized in the analysis of SEC solvent systems where non-aggregated polymers showed a monomodal peak on the size distribution chromatograph. Aggregation was not observed in the aqueous SEC solvent consisting of 0.7 M sodium nitrate and 0.1 M Tris adjusted to pH 6.0 with glacial acetic acid; however

interactions between the nucleobase groups and the SEC columns led to tailing in the chromatograph and inaccurate molecular weight analysis.

2.4.2 Effect of the incorporation of nucleobase-containing groups on the thermal properties of PDMAEMA.

The thermal properties of the nucleobase-containing polyelectrolytes were investigated using differential scanning calorimetry (DSC) and thermogravimetric analysis (TGA). The onset of thermal degradation for the both the neutral and protonated species of both poly(9-VBA–*co*–DMAEMA) and poly(1-VBT–*co*–DMAEMA) were measured to be above 250 ºC by TGA. The initial degradation mechanism is attributed to the Hoffmann elimination of the DMAEMA side chain. Glass transition temperatures determined using DSC for poly(9-VBA–*co*–DMAEMA) ranged from 42 ^{o}C to 122 ^{o}C for the neutral copolymers (Figure 2.7) and 170 ^{o}C to 188 ^{o}C for the protonated copolymers. Glass transition temperatures for these copolymers are summarized in Table 2.1.

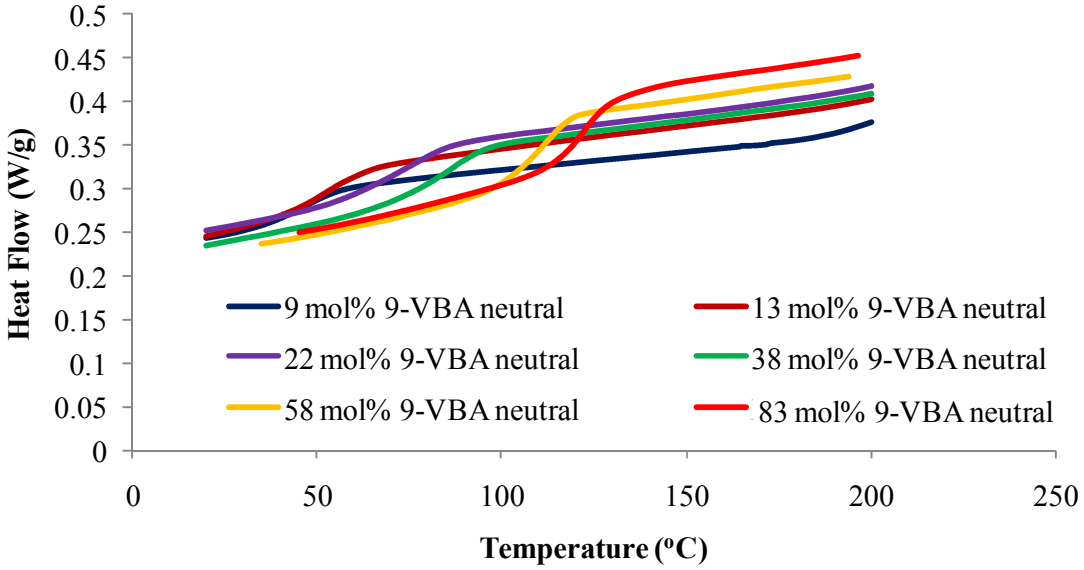

Figure 2.6. DSC plots for neutral poly(9-VBA–*co*–DMAEMA)

Table 2.1. Glass transition temperatures for nucleobase-containing copolymers

	T_g (neutral)	T_g (charged)
9 mol% 9-VBA	42 °C	170 °C
13 mol% 9-VBA	68 °C	172 °C
22 mol% 9-VBA	78 °C	174 °C
38 mol% 9-VBA	98 °C	182 °C
58 mol% 9-VBA	113 °C	186 °C
83 mol% 9-VBA	122 °C	188 °C
9 mol% 1-VBT	45 °C	166 °C
20 mol% 1-VBT	53 °C	167 °C
33 mol% 1-VBT	76 °C	168 °C
47 mol% 1-VBT	87 °C	171 °C

An increase in the glass transition temperature is observed for both neutral and protonated poly(9-VBA–*co*–DMAEMA) with increased amounts of 9-VBA in the polymer composition. The observed increase in the glass loosely follow the trend defined by the Fox copolymer glass transition equation: $\frac{1}{Tg} = \frac{w_a}{Tg,_a} + \frac{w_b}{Tg,_b}$. In this equation, the T_g of the copolymer is calculated from the weight fraction of each monomer and the T_g of each homopolymer (Figure 2.8).

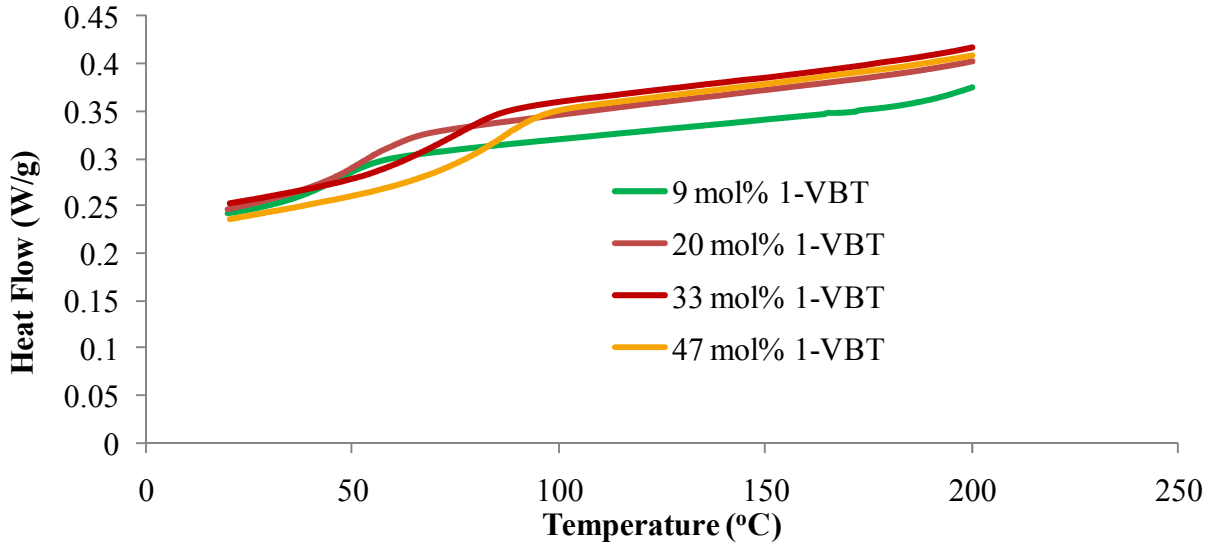

Figure 2.7. DSC plots for neutral poly(1-VBT–*co*–DMAEMA)

Glass transition temperatures determined by DSC for poly(1-VBT–*co*–DMAEMA) also follow the trend defined with the Fox copolymer equation (Figure 2.8). The T_g values range from 45 ^oC to 83 ^oC for the neutral copolymers and from 166 ^oC to 171 ^oC for the protonated samples (Table 2.1). For both of the nucleobase-containing copolymer series the significant increase in T_g observed upon protonation of the DMAEMA groups is due to the electrostatic interactions between the polymer chains leading to a decrease in chain mobility. Long range segmental motion cannot occur until the dissociation temperature for these electrostatic interactions is reached. Hydrogen bonding interactions between the nucleobases is also believed to form a thermally-labile dynamic network structure in these copolymers.

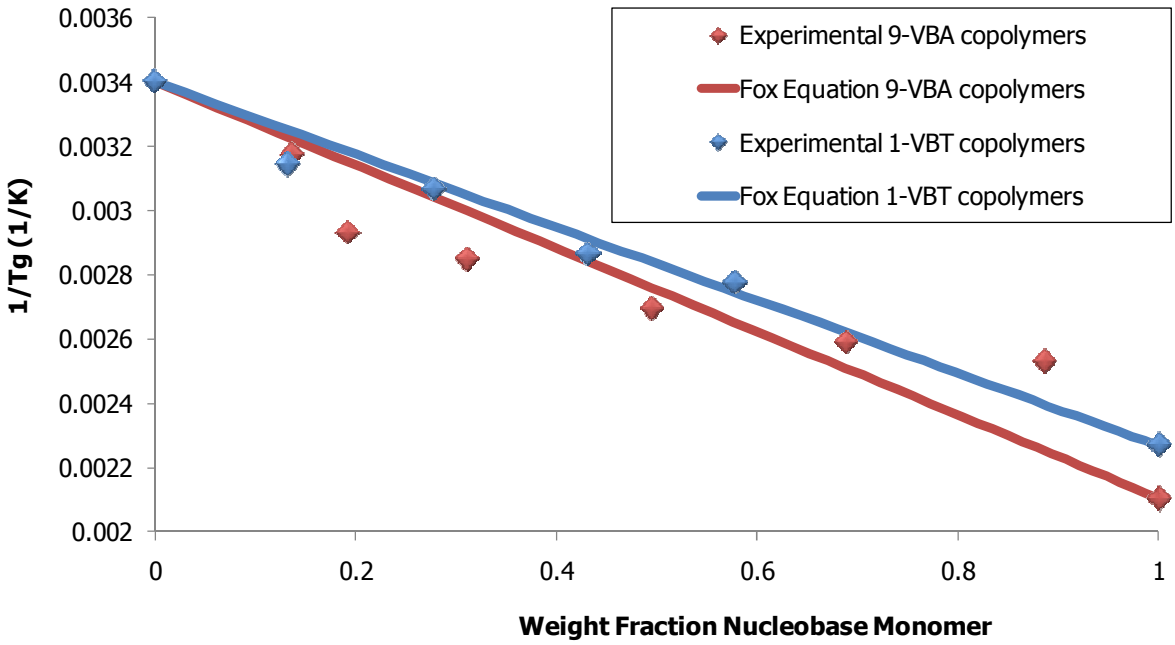

Figure 2.8. Fox equation and experimental glass transition temperatures

2.4.3 Mayo-Lewis determination of the monomer reactivity ratios for the synthesis of poly(9-VBA–*co*–DMAEMA).

A series of nucleobase-containing polyelectrolytes containing various amounts of hydrogen bonding groups was synthesized; however it was observed that the polymerization process yielded a higher mole fraction than was charged into the reaction flask (Table 2.2). This observation prompted investigation into the reactivity ratios between 9-VBA and DMAEMA in order to explain this trend.

Table 2.2. 9-VBA mol% in feed vs. in polymer composition

9-VBA mol% in feed	9-VBA mol% from NMR
5	9
9	13
16	22
23	38
33	58

The reactivity ratios of two monomers are determined with the equations:

$$r_1 = \frac{k_{11}}{k_{12}} \qquad r_2 = \frac{k_{22}}{k_{21}}$$

The rate constants k_{11} and k_{12} describe the propagation of the growing polymer chain having monomer 1 as the reactive end group with monomer 1 and 2 respectively, while k_{22} and k_{21} describe the addition of the monomers to the polymer chain ending in monomer 2. The Mayo-Lewis determination of reactivity ratios utilizes a linear form of the copolymer equation:[32]

$$r_1 = r_2\left(\frac{d[M_1] * [M_2]^2}{d[M_2] * [M_1]^2}\right) + \frac{[M_2]}{[M_1]}\left(\frac{d[M_1]}{d[M_2]} - 1\right)$$

One method previously reported by Long et al shows the determination of $r_2\left(\frac{d[M_1]*[M_2]^2}{d[M_2]*[M_1]^2}\right)$ and $\frac{[M_2]}{[M_1]}\left(\frac{d[M_1]}{d[M_2]} - 1\right)$, the slope and intercept respectively, from data produced from a number of copolymerizations monitored with *in situ* FTIR spectroscopy.[33]

In Situ FTIR was utilized in monitoring the polymerization of 9-VBA and DMAEMA in various mole ratios and in the determination of the reaction kinetics. These polymerizations were performed as described in the Experimental; however a two neck round-bottomed flask was utilized to allow for immersion of the *in situ* FTIR probe into the reaction solution. The disappearance of 9-VBA was monitored by measuring the absorbance at 998 cm^{-1} while the disappearance of DMAEMA was monitored at 1167 cm^{-1} (Figure 2.9). In both cases the absorbencies were well resolved and a peak to two-point baseline was used to quantitatively determine the decrease in the area underneath the peaks.

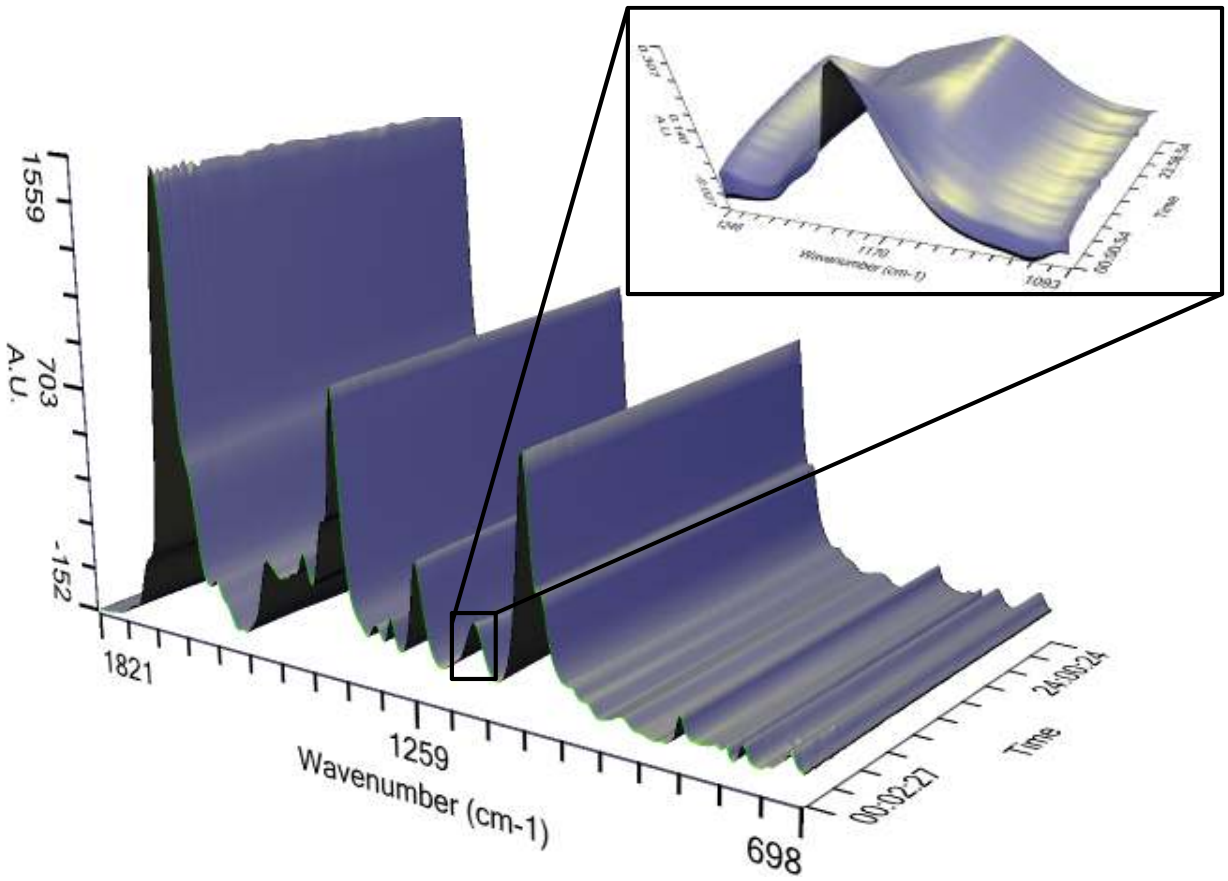

Figure 2.9. Waterfall plot of DMAEMA monomer C-O stretch disappearance with the synthesis of poly(9-VBA–*co*–DMAEMA)

Converting the relative absorbance of each peak to normalized concentration of monomer allowed for determination of the kinetics for the copolymerization reaction (Figure 2.10). Both monomers show approximately 60% conversion, which is typical for free-radical polymerization reactions.

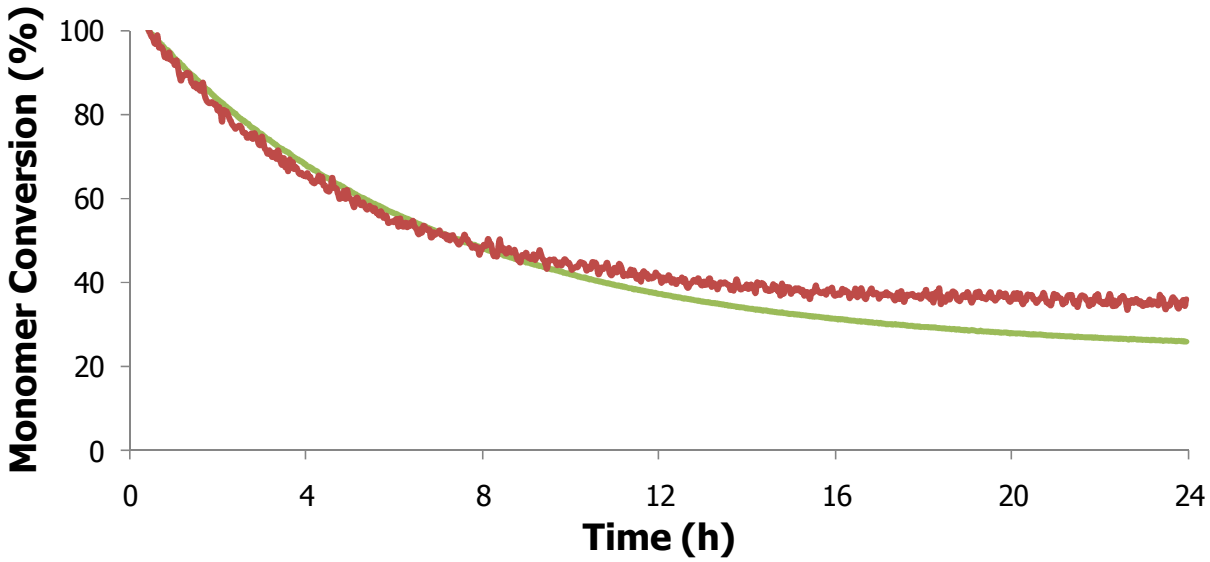

Figure 2.10. Reaction kinetics for synthesis of poly(9-VBA–*co*–DMAEMA)

Determination of d[VBA]/d[DMAEMA] was achieved with analysis of the reaction kinetics for each polymerization for only the first ten percent conversion of the monomers to ensure accuracy the monomer concentrations throughout the range used for reactivity ratio calculations as well as linearity of the data plots (Figure 2.11). The slope of the plot of the normalized concentration of DMAEMA vs. the normalized concentration of 9-VBA gave the value of d[VBA]/d[DMAEMA] for each of the copolymerization reactions shown in Table 2.3.

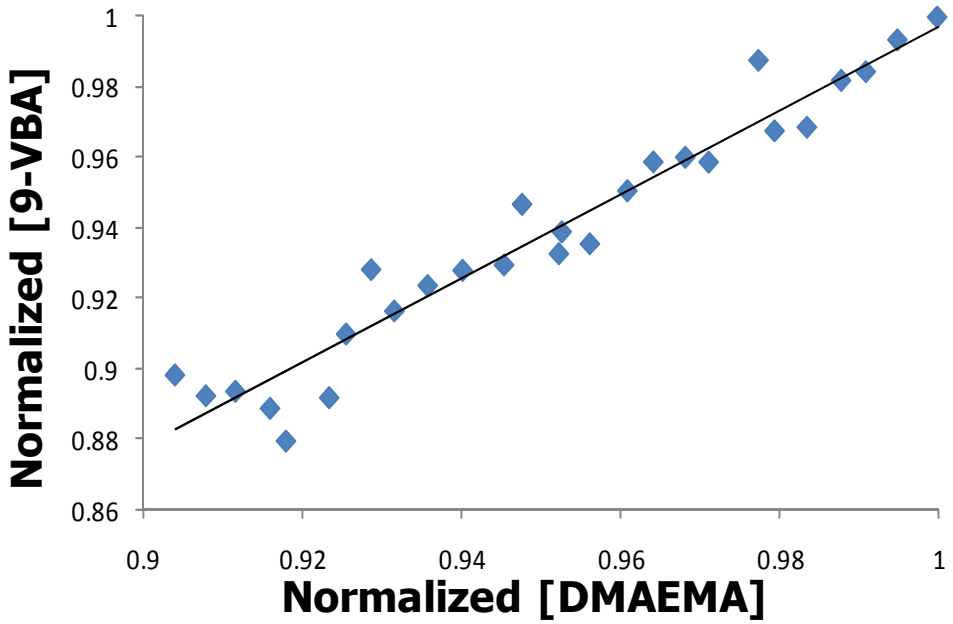

Figure 2.11. Determination of d[VBA]/d[DMAEMA] from *in situ* FTIR spectroscopy reaction kinetics data

Table 2.3. d[VBA]/d[DMAEMA] values as calucated from *in situ* FTIR spectroscopy reaction kinetics data

VBA:DMAEMA	[VBA]/[DMAEMA]	d[VBA]/d[DMAEMA]
25/75	**3.00**	**1.18**
35/65	**1.87**	**1.38**
45/55	**1.22**	**1.65**

The linear form of the copolymer composition equation for the polymerization of 9-VBA and DMAEMA is as follows:

$$r_{9-VBA} = r_{DMAEMA}\left(\frac{d[M_{9-VBA}] * [M_{DMAEMA}]^2}{d[M_{DMAEMA}] * [M_{9-VBA}]^2}\right) + \frac{[M_{DMAEMA}]}{[M_{9-VBA}]}\left(\frac{d[M_{9-VBA}]}{d[M_{DMAEMA}]} - 1\right)$$

This equation can be utilized once the values of d[VBA]/d[DMAEMA] are determined. Subsituting values ranging from -1 to 1 for $r_{9\text{-VBA}}$ gives a range of values for r_{DMAEMA} for

each copolymerization. The assumed values of $r_{9\text{-VBA}}$ and the calculated values of r_{DMAEMA} are then

plotted for each of the polymerization reactions as shown in Figure 2.12.

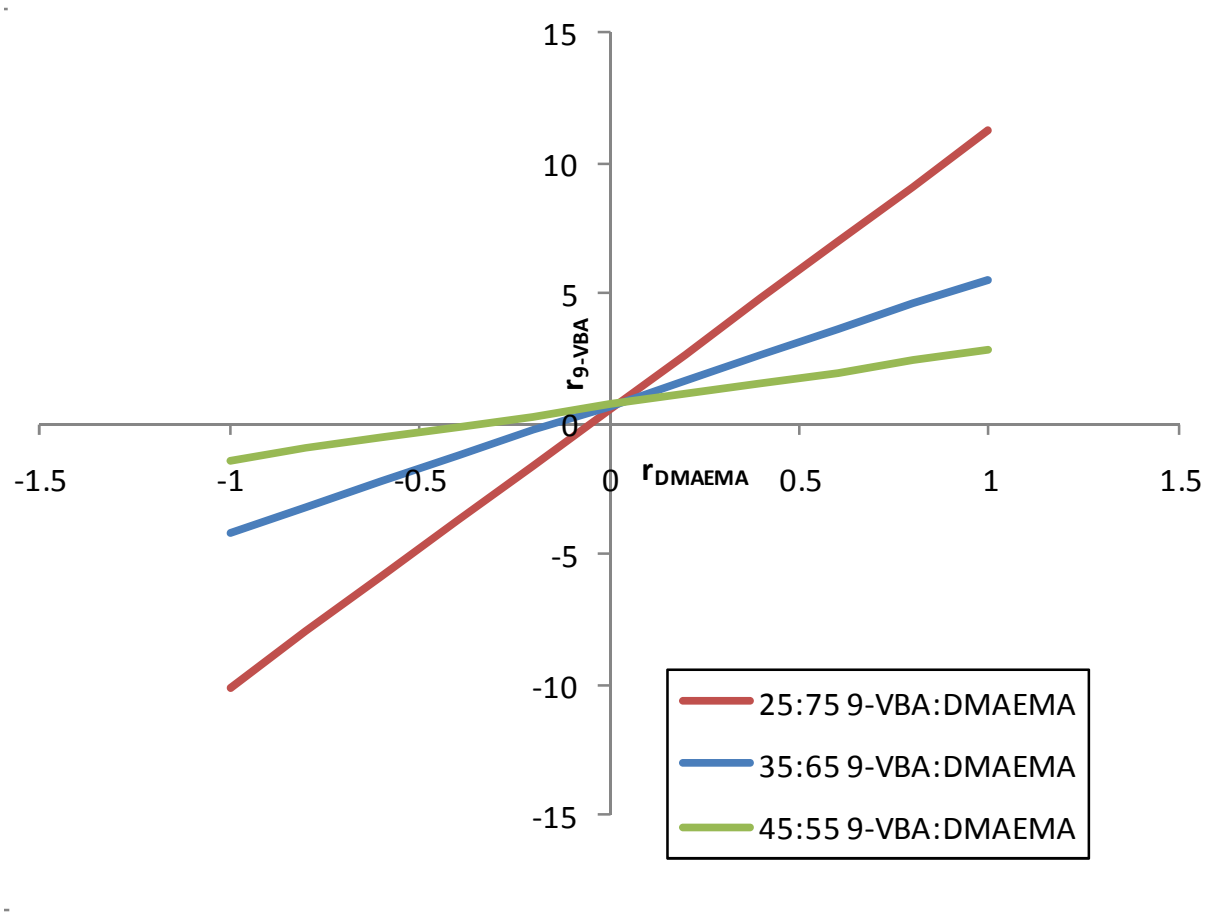

Figure 2.12. Mayo-Lewis determination of the reactivity ratios for 9-VBA and DMAEMA

The intersection of the lines in this plot gives the experimental values of $r_{9\text{-VBA}}$ and r_{DMAEMA}. The x-coordinate for the point of intersection corresponds to the value for $r_{9\text{-VBA}}$ while the y-coordinate corresponds to the value for r_{DMAEMA}. The calculated values of r_{VBA} and r_{DMAEMA} are 0.75 and 0.03, respectively. These results indicate the 9-VBA radical chain end slightly prefers to react with the DMAEMA monomer while the

DMAEMA radical chain end preferentially reacts with the 9-VBA monomer. With an r_1r_2 value close to zero the polymer composition is assumed as mainly alternating.

2.4.4 Salt-triggering with poly(9-VBA-co-DMAEMA)

The charge density, condensation of the counterions, and the phase separation behavior of polyelectrolytes are the determining factors for solubility in monovalent salt solutions. Four stages of solubility of polyelectrolytes in aqueous solutions are previously reported. Polyelectrolytes in the first stage are described as having an extended rod-like conformation, a state typically observed in pure water. The formation of ion-bridging between two ionic sites on the polymer backbone and divalent counterions defines the second stage in which the polymer remains soluble in the aqueous solution. A solubility transition is observed in the third stage of solubility in aqueous solutions, due to high levels of charge screening the polyelectrolyte precipitates out of solution, which is termed "salting out". In the last stage, stage four, a further increase in salt concentration leads to the polyelectrolyte redissolving in the aqueous solution, which is known as "salting in". It is previously reported that PDMAEMA will undergo both "salting in" and "salting out" with aqueous solutions containing varying concentrations of NaI.

Investigation into the salt-triggerability of nucleobase-containing PDMAEMA was performed using both a 5 wt% (0.85 M) NaCl solution in deinonized water and in pure deionized water. Poly(9-VBA–*co*–DMAEMA) was dissolved in the aqueous solvents to give 1 mg/mL solutions. The solutions were carefully mixed for thirty minutes, at which time the insoluble mixtures were heated with a heat gun for several minutes. Table 2.4 summarizes the solubilities of each polymer composition in the two

aqueous solvents. In the case of both samples containing the highest mole% 9-VBA the polymer became dispersed in the NaCl solution, however the solution never became optically clear and the polymer formed a film on the bottom of the vial upon cooling (Figure 2.13).

Figure 2.13. Protonated poly(9-VBA–*co*–DMAEMA) in water (right) and NaCl solution (left)

Table 2.4. Salt triggerability of protonated poly(9-VBA–*co*–DMAEMA)

	di H_2O	5 wt% NaCl in di H_2O
22 mole% 9-VBA	Optically clear	Optically clear when heated
38 mole% 9-VBA	Optically clear	Optically clear when heated
58 mole% 9-VBA	Optically clear	Insoluble
83 mol% 9-VBA	Optically clear	Insoluble

The salt-triggering effect observed for poly(9-VBA–*co*–DMAEMA) prompted further investigation into the structure-property relationship of solubility for these polymers. A PDMAEMA copolymer containing 60 mol% styrene was synthesized as a control for this polymer. The solubility of protonated poly(styrene–*co*–DMAEMA) was explored with the same method as employed for the poly(9-VBA–*co*–DMAEMA) polymers. It was observed that the copolymer lost its salt triggerability in the absence of the nucleobase group (Figure 2.14).

Figure 2.14. Protonated poly(styrene–*co*–DMAEMA) in water (right) and NaCl solution (left)

One hypothesis for the observed effects of incorporation of nucleobases into the polymer structure is that the charge screening observed in polyelectrolyte salt solutions brought the hydrogen-bonding groups in closer proximity to each other, encouraging formation of intermolecular associations through these groups. Even though water is a competitive solvent, meaning that is will form hydrogen bonding interactions with the nucleobases and prevent association of these nucleobases with each other; the increased proximity of the polymer chains and the higher association constants for nucleobase pairing encourages formation of these bonds.

2.4.5 Solution rheology of poly(9-VBA-co-DMAEMA)

Polyelectrolytes exhibit an extended, rod-like conformation in dilute aqueous solutions, which is due to charge repulsion between pendant charges along the polymer backbone and the rearrangement of counterions in solution. Four concentration regimes exist for polymer solutions[34]. The fist regime is defined where the concentration is below C*, the transition between the dilute and semi-dilute regimes, and is characterized with widely separated polymer chains. The second concentration regime exists between C*

and C_e, the entanglement concentration. In these concentrations the polymer chains begin to touch but do not yet entangle. In the third regime the concentration is above C_e and below C_D, the drag coefficient where the transition to the concentrated regime is reached. In these concentrations the overlap of polymer chains restricts chain mobility. Above C_D the chain dimensions are independent of concentration. Limited solution rheology studies were performed on adenine-containing PDMAEMA with a 9-VBA:DMAEMA molar ratio of 5:95 in order to determine the scaling relationship between specific viscosity and concentration. Figure 2.15 shows a plot of the zero shear viscosity versus polymer concentration. Concentrations ranging from 2 to 20 wt% polymer in deionized water were tested.

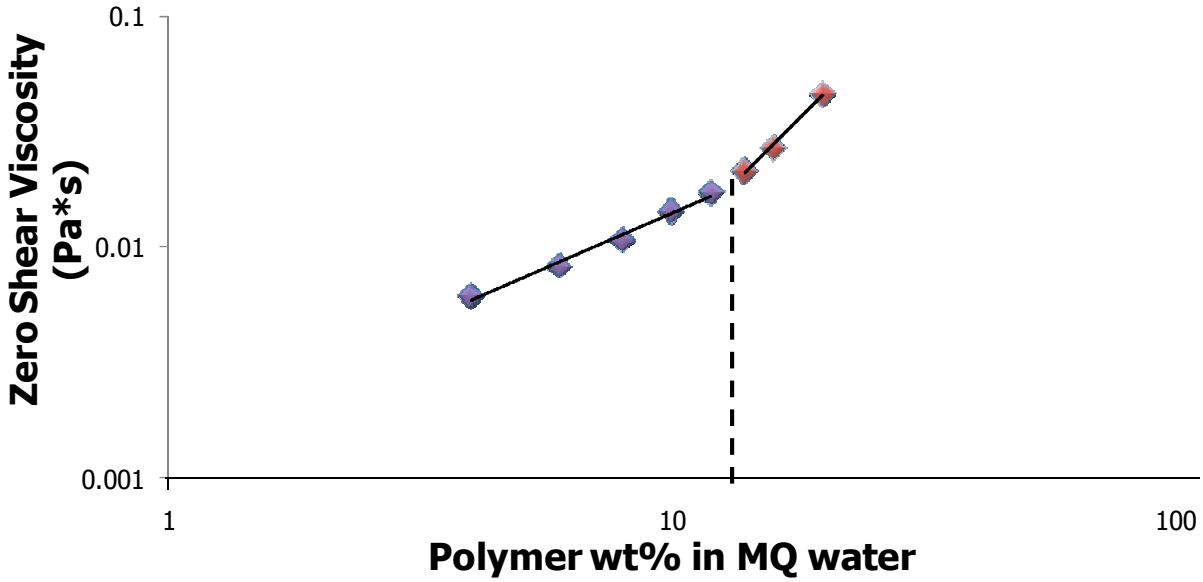

Figure 2.15. Solution Rheology of protonated poly(9-VBA–*co*–DMAEMA) in water

The scaling relationship of the 9-VBA copolymer below C_e was calculated as 0.94, which is slightly higher than that for a PDMAEMA.HCl homopolymer which has a scaling relationship of 0.8. Above C_e the scaling relationship for the copolymer is 2.2 while the

homopolymer scaling relationship is 1.7. These results suggest the incorporation of the nucleobase monomer into the polymer composition may lead to an increase in the scaling relationships, however further investigation using higher molar ratios of 9-VBA would allow for more definite conclusions on this relationship.

2.5 Conclusions

Nucleobase-containing PDMAEMA copolymers were shown to be thermally stable to 250 ^{o}C and to show glass transition temperatures following the Fox equation. *In situ* FTIR analysis of the polymerization revealed the reaction reaches completion after 24 hours and allowed for analysis of the reaction kinetics as well as determination of the reactivity ratios using the Mayo-Lewis determination method. Solubility of the copolymers was significantly affected upon incorporation of the styrenic nucleobases and prevented molecular weight analysis using SEC. The solubility of these copolymers on aqueous solutions was also significantly affected upon incorporation of the nucleobases and showed salt-triggerability with higher contents of these groups. Solution rheology also revealed the influence of hydrogen bonding on the apparent viscosity and entanglement concentrations of these polyelectrolytes.

2.6 Acknowledgements

We would like to acknowledge Shijing Cheng and Dr. Philippe Bissel for helpful discussions and assistance with monomer synthesis. We would also like to acknowledge Matthew Hunley for assistance with solution rheology measurements and Matt Green for assistance with dynamic light scattering.

2.7 References

(1) Cheng, C. C.; Huang, C. F.; Yen, Y. C.; Chang, F. C. *J. Polym. Sci. Pol. Chem.* **2008**, *46*, 6416.
(2) Beijer, F. H.; Kooijman, H.; Spek, A. L.; Sijbesma, R. P.; Meijer, E. W. *Angew. Chem.-Int. Edit.* **1998**, *37*, 75.
(3) Binder, W. H.; Zirbs, R. In *Hydrogen Bonded Polymers*; Springer-Verlag Berlin: Berlin, 2007; Vol. 207, p 1.
(4) Lawrence, D. S.; Jiang, T.; Levett, M. *Chem. Rev.* **1995**, *95*, 2229.
(5) Lehn, J. M. In *Conference on Polymers in the 3rd Millennium*; Polymer Int, I. D., Electr Insulat Soc, I. A. E., Sism, W. I. D., Eds.; John Wiley & Sons Ltd: Montpellier, France, 2001, p 825.
(6) Mather, B. D.; Baker, M. B.; Beyer, F. L.; Berg, M. A. G.; Green, M. D.; Long, T. E. *Macromolecules* **2007**, *40*, 6834.
(7) Mather, B. D.; Baker, M. B.; Beyer, F. L.; Green, M. D.; Berg, M. A. G.; Long, T. E. *Macromolecules* **2007**, *40*, 4396.
(8) Mather, B. D.; Elkins, C. L.; Beyer, F. L.; Long, T. E. *Macromolecular Rapid Communications* **2007**, *28*, 1601.
(9) Williams, S. R.; Mather, B. D.; Miller, K. M.; Long, T. E. *Journal of Polymer Science Part a-Polymer Chemistry* **2007**, *45*, 4118.
(10) Lutz, J.-F.; Pfeifer, S.; Chanana, M.; Thuenemann, A. F.; Bienert, R. *Langmuir* **2006**, *22*, 7411.
(11) Mather, B. D.; Baker, M. B.; Beyer, F. L.; Berg, M. A. G.; Green, M. D.; Long, T. E. *Macromolecules (Washington, DC, United States)* **2007**, *40*, 6834.
(12) Sivakova, S.; Rowan, S. J. *Chemical Society Reviews* **2005**, *34*, 9.
(13) Hoogsteen, K. *Acta Crystallographica* **1963**, *16*, 907.
(14) Sundaralingam, M. *Int. J. Quantum Chem.* **1977**, 11.
(15) Arnott, S.; Bond, P. J.; Selsing, E.; Smith, P. J. C. *Nucleic Acids Res.* **1976**, *3*, 2459.
(16) Sivakova, S.; Rowan, S. J. *Chem. Soc. Rev.* **2005**, *34*, 9.
(17) Sedlak, M.; Simunek, P.; Antonietti, M. *J. Heterocycl. Chem.* **2003**, *40*, 671.
(18) Srivatsan, S. G.; Parvez, M.; Verma, S. *Chem.-Eur. J.* **2002**, *8*, 5184.
(19) Srivatsan, S. G.; Verma, S.; Parvez, M. *Acta Crystallographica Section C-Crystal Structure Communications* **2002**, *58*, o378.
(20) Yang, X. P.; Xu, P. S.; Ding, S. J.; Radosz, M.; Shen, Y. Q. In *227th ACS National Meeting*; Amer Chemical Soc: Anaheim, CA, 2004, p POLY.
(21) Lutz, J.-F.; Thuenemann, A. F.; Nehring, R. *Journal of Polymer Science, Part A: Polymer Chemistry* **2005**, *43*, 4805.
(22) Jorgensen, W. L.; Pranata, J. *J. Am. Chem. Soc.* **1990**, *112*, 2008.
(23) Krische, M. J.; Lehn, J. M. In *Molecular Self-Assembly* 2000; Vol. 96, p 3.
(24) Lehn, J. M. In *4th European Polymer Federation Symp on Polymeric Materials*; Huthig & Wepf Verlag: Baden Baden, Germany, 1992, p 1.
(25) Lehn, J. M. In *Conference on the Nato Advanced Research Workshop on Supramolecular Science - Where It is and Where It is Going*; Ungaro, R. D. E., Ed.; Springer: Lerici, Italy, 1998, p 287.
(26) Reinhoudt, D. N.; Stoddart, J. F.; Ungaro, R. *Chem.-Eur. J.* **1998**, *4*, 1349.

(27) Lutz, J.-F.; Thuenemann, A. F.; Rurack, K. *Macromolecules* **2005**, *38*, 8124.
(28) Elkins, C. L.; Park, T.; McKee, M. G.; Long, T. E. *Journal of Polymer Science Part a-Polymer Chemistry* **2005**, *43*, 4618.
(29) Layman, J. M.; Ramirez, S. M.; Green, M. D.; Long, T. E. *Biomacromolecules* **2009**, *10*, 1244.
(30) McKee, M. G.; Hunley, M. T.; Layman, J. M.; Long, T. E. *Macromolecules* **2006**, *39*, 575.
(31) Deng, L.; Wang, C. H.; Li, Z. C.; Liang, D. H. *Macromolecules* **2010**, *43*, 3004.
(32) Mayo, F. R.; Lewis, F. M. *Journal of the American Chemical Society* **1944**, *66*, 1594.
(33) Wilkes, K. B.; Bhanu, V. A.; A.J., P.; Long, T. E.; McGrath, J. E. *Journal of Polymer Science: Part A: Polymer Chemistry* **2004**, *42*, 2994.
(34) Don, S. C.; Colby, R. H. *Macromolecules* **2008**, *41*, 6505.

Chapter 3. Gene delivery with adenine- and thymine-containing PDMAEMA

3.1 Abstract

Polyelectrolytes are capable of binding and condensing DNA through electrostatic interactions with the negatively charged phosphate groups of the DNA backbone. The condensed particles, termed polyplexes, are then capable of passing though the cell membrane in a process known as endocytosis. Once the polyplex has entered the cell the polyplex dissociates, allowing the DNA to enter the nucleus and undergo transcription and translation so that the cellular machinery can produce the protein for which the DNA is encoded for. Synthetic polyelectrolytes show high transfection efficiencies; however a high degree of cytotoxicity is also often observed for these gene delivery vectors. The high level of cytotoxicity is attributed to high degree of cationic character for the polyplexes formed with these vectors according to the proton-sponge hypothesis. One method of reducing the overall cationic character for these vectors is incorporation of non-electrostatic binding mechanisms such as hydrogen bonding. A series of nucleobase-containing PDMAEMA copolymers were synthesized in order to investigate the effect of incorporation of these groups on the cell viability, binding efficiency, and transfection efficiency of PDMAEMA. Incorporation of sytrenically linked nucleobases significantly reduced the solubility of PDMAEMA so only copolymers containing low amounts of the nucleobases were able to be analyzed. Results from the MTT cell viability assay, DNA binding gel-shift assay, and the luciferase expression gene transfection assay suggest the incorporation of hydrogen bonding groups and reduction of the overall cationic character of PDMAEMA does not affect the cytotoxicity of these vectors, however the ratio of hydrogen bonding groups to protonated amine from PDMAEMA is quite low and could explain why more of an effect was not observed.

3.2 Introduction

One synthetic polycation that is widely investigated for its possible applications as a gene delivery vector is poly(2-(dimethylamino)ethyl methacrylate) (PDMAEMA).[1-7] Other cationic polymers have shown higher transfection efficiencies as compared to PDMAEMA, however because the synthetic strategies and biological characterization of PDMAEMA is well established it is an ideal vector for investigating the effect of incorporation of hydrogen bonding groups with the structure-transfection studies. PDMAEMA (Figure 3.1) is reported to effectively condense pDNA through electrostatic interactions when protonated at physiological pH.[1] The resulting polyplexes show a small distribution of sizes and slight cationic character that are capable of demonstrating high transfection efficiencies.[1]

Figure 3.1. Protonated and neutral forms of PDMAEMA [1-3]

Transfection studies of luciferase-encoded pDNA into COS-7 cells reveal a strong relationship between transfection efficiencies and the molecular weight of the polycation.[3] Layman et al. showed that gene expression increases significantly as a function of increasing molecular weight; however molecular weight was not shown to influence cellular uptake of polyplexes formed with these vectors. Even though it was shown that condensed pDNA particles with a smaller average diameter were attained with high molecular weight PDMAEMA as compared to low molecular weight polymers, no correlation was shown with polyplex diameter and transfection efficiency.[3]

It is hypothesized that the polyplex diameter influences the increased transfection efficiencies because of the increased cellular uptake observed for smaller particle sizes.[3] Particles smaller than 200 nm typically enter through the clathrin-mediated pathway while larger particles typically enter through the caveolae mediated mechanism.[8] The exact mechanism of cellular uptake is not well understood for these polyplexes.[3,7,9,10]

Current research suggests that endocytosis is the method of cellular uptake of these polyplexes.[11] Studies of the intracellular trafficking of the polyplexes utilized fluorescent labels. Transfection studies of COS-7 cells with PDMAEMA demonstrated two cellular uptake routes, the clathrin-dependant and the caveolae-dependant pathways.[11] Inhibition of either pathway resulted in a minimal decrease in uptake of the polyplexes indicating that polyplexes undergo either mechanism.[11] Although cellular uptake was consistent regardless of pathway inhibition, a significant decrease in transfection efficiencies was observed upon inhibition of the caveolae-mediated uptake route.[11] This effect is attributed to the dynamic nature of the endocytic pathways.[8,11] Inhibition of one pathway often results in an increase in polyplex uptake via a mechanism that is not experimentally regulated.[11]

Layman et al. suggested the intercellular fate of PDMAEMA base polyplexes showed a more significant influence of transfection efficiencies than the mechanism of cellular entry.[3] It is suggested that the process of intercellular trafficking plays a key role in the transfection efficiency of these vectors, which is highly dependent on the binding affinity between the polymer and pDNA. Incorporation of non-electrostatic binding mechanisms can influence these binding efficiencies. Prevette et al. showed the determination of the binding mechanism between pDNA and the PGAA gene delivery agents provides a great deal of information concerning the structure-property relationships of these vectors, specifically concerning the importance of the

hydrogen bonding interactions.[12] The importance of hydrogen bonding interactions was also confirmed in vectors based on PGAAs, which showed both electrostatic and non-electrostatic interactions upon formation of the polyplex. These results suggest that incorporation of strong hydrogen bonding motifs into the polymeric structure could reduce or eliminate the necessity of the cationic character of previously investigated non-viral gene delivery agents, which is hypothesized to significantly decrease the cytotoxicity observed in current cationic polyelectrolyte vectors. Hydrophobic interactions were shown to play an inconsequential role in the formation of the polyplexes; however differences in the free binding energies when the only structural variation is the quantity and stereochemistry of hydroxyl functional groups from the carbohydrate group suggests the significance of hydrogen bonding interactions in the binding affinities of these polymers structures.[12]

Incorporation of nucleobase hydrogen bonding groups into the PDMAEMA structure is expected to take advantage of well established binding motifs between nucleic acid bases. While bound to the double helix structure of dsDNA these base pairs demonstrate the ability to act as both hydrogen bond donors and acceptors.[13] Hoogsteen base pair interactions allow for triplex DNA formation in the DNA minor groove.[14] It is hypothesized that polyplex formation with these vectors will initiate through electrostatic interactions and binding affinity enhancement will occur due to hydrogen bonding interactions between the polymer chain and the dsDNA.

3.3 Experimental

3.3.1 Materials.

Adenine (99%) was purchased from Aldrich. 4-vinylbenzyl chloride (90%) purchased from Fluka. Potassium carbonate (99%) was purchased from Aldrich. 2-(*dimethylamino)ethyl methacrylate* (98%) was purchased from Aldrich. Methanol (99.9%), dimethyl sulfoxide (99.9%), chloroform (99.9%), and *N,N*-dimethylformamide (99.5%) were purchased from Fisher. Triethyl amine was purchased from Aldrich.

3.3.2 Instrumentation.

^{1}H NMR spectroscopic data was collected in DMF-d_7, DMSO-d_6, and D_2O on a Varian 400 MHz spectrometer. Differential Scanning Calorimetry (DSC) was obtained with TA DSC Instruments under nitrogen at a heating and cooling rate of 10 ºC/min. Values from the second heating were reported. Thermogravimetric analysis (TGA) was performed on a TA Instruments TGA under a nitrogen atmosphere at a heating rate of 10°C/min.

3.3.3 Cell culture.

COS-7 were isolated, cultivated, and purified as previously described. COS-7 were cultured in RPMI 1640-based medium with 10% fetal bovine serum (Mediatech), 10% NuSerum (Becton Dickinson), 30 μg/mL of endothelial cell growth supplement (ECGS; Becton Dickinson), 15 U/mL of heparin (Sigma, 2 mM L-glutamine, 2 mM sodium pyruvate, nonessential amino acids, vitamins, 100 U/mL of penicillin, and 100 μg/mL of streptomycin (all reagents from Mediatech). Cultures were incubated at 37 °C in a humid atmosphere of 5% CO_2.

3.3.4. DNA shift assay.

Polyplexes were prepared in 1X TAE buffer by addition of varying concentrations of polymer solution to DNA solution. The polyplex and DNA only solutions were incubated for 30 min at room temperature. To the solutions was added 7 μL of a 40 wt % sucrose, 0.3 w/v% bromophenol blue in 1× TAE loading buffer solution proir to loading in submerged agarose slabs. Agarose powder (BioRad Laboratories) was dissolved in hot 1× TAE buffer containing 1× SYBR Green I (Sigma) to produce 0.9 wt % agarose gel slabs. The gel was electrophoresed at 75 V for 35 min in 1× TAE buffer and imaged using a UV transilluminator table and a digital camera equipped with a hood and green filter.

3.3.5. Cell viability assay.

Cell viability was determined using the 3-[4,5-dimethylthiazol-2-yl]2,5-diphenyltetrazolium bromide (MTT, Sigma-Aldrich) conversion assay. Each polymer sample was dissolved at 1 mg/mL in phosphate buffered saline. Then, 25-250 μL of 1 mg/mL polymer solution was diluted in 5 mL of basal RPMI 1640 yielding treatment solutions ranging 5-50 μg/mL. Cells were plated at 5 x10^4 cells/mL in a 96-well plate and incubated for 24 hours (37 ^{o}C, 5% CO_2). The cells were washed with 1X HBSS. Polymer solutions of varying concentrations in serum-free media were added and incubated for 12 hours (37 ^{o}C, 5% CO_2). The cells were then washed with 1X HBSS and a 0.5 mg/mL solution of MTT in basal media was added and incubated for four hours (37 ^{o}C, 5% CO_2). After four hours, the solutions were aspirated. DMSO was then added to solubilize the formazan product, and visualized at 570 nm using a Molecular Devices Corp. SPECTRAmax M2 microplate reader following 30 minutes of rocking.

3.3.6. Luciferase expression assay.

To prepare polyplexes for transfection experiments, gWiz-Luc plasmid (1 μg/μL in H2O) was diluted in basal RPMI media to a concentration of 0.8 μg/mL and incubated at room temperature for 10 min. At the same time, the appropriate type and amount of polymer was diluted in basal RPMI to the final concentrations corresponding to the various nitrogen/phosphorus (N/P) ratios and allowed to incubate for 10 min at room temperature. Equal volumes of the plasmid and corresponding polymer solutions were combined (final pDNA concentration of 0.4 μg/mL) and incubated for 20-30 min at room temperature to complex the plasmid DNA with each polymer composition. COS-7 cells were plated at a concentration of 2.0×10^5 cells/well on 12-well plates 24 h prior to transfection. Each well was treated with 1 mL of transfection solution and then incubated for 12 h at 37 °C, 5% CO_2. After 12 h, the transfection solution was replaced with complete RPMI growth media. The cells were then incubated for 24 h at 37 °C, 5% CO_2 to allow for protein expression. After incubation, the cells were rinsed with approximately 1 mL of PBS and 100 μL of lysis buffer was added. Immediately after adding lysis buffer the plates were incubated for 30 min at room temperature with gentle mixing. The lysate mixture was then subjected to two -80 °C/37 °C freeze/thaw cycles. Luciferase activity was measured using a luciferase assay kit (Promega) and a Molecular Devices Corp. SPECTRAmax L luminometer according to the assay kit manufacturer's instructions.

3.4 Results and discussion

3.4.1 Solubility effects of incorporation of nucleobase-containing groups with PDMAEMA

The goal was to synthesize a series of nucleobase-containing copolymers with 9-VBA or 1-VBT and DMAEMA to investigate the influence of the incorporation of hydrogen bonding groups on the gene delivery efficiency of PDMAEMA. One major obstacle that was encountered was the effect of the incorporation of the styrenic nucleobases on the solubility of PDMAEMA. The nucleobases adenine and thymine are not water soluble and the styrene linker does not afford any significant increase in solubility. Copolymers of DMAEMA and these nucleobase-containing monomers show salt-triggerability in aqueous solutions as discussed in section 2.4.4. Similar effects are observed in the phosphate-buffered solution (PBS) utilized in the biological assays performed in sections 3.4.2 through 3.4.4. Copolymers containing lower mole percents of 9-VBA are optically clear while the copolymer containing 58 mol% 9-VBA yields a cloudy solution as shown in Figure 3.2.

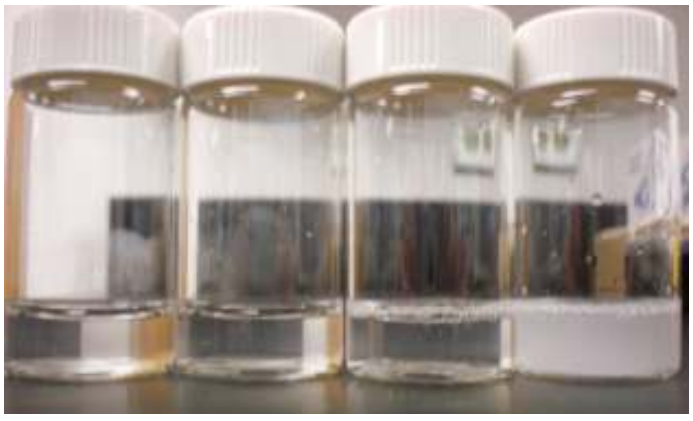

Figure 3.2. 1mg/mL solutions of poly(9-VBA–*co*–DMAEMA) in PBS containing 13, 22, 38, and 58 mol% 9-VBA (left to right)

Further investigation into the solubility of these copolymers is PBS utilized dynamic light scattering (DLS). Since the solutions are filtered through a sterile syringe filter it is important to ensure that aggregation of the polymer is minimal. DLS traces for the optically clear showed significant aggregation for the copolymers containing 13 and 22 mol% 9-VBA. The size distribution by intensity trace of the 9 mol% 9-VBA copolymer also showed aggregation as seen in Figure 3.3.

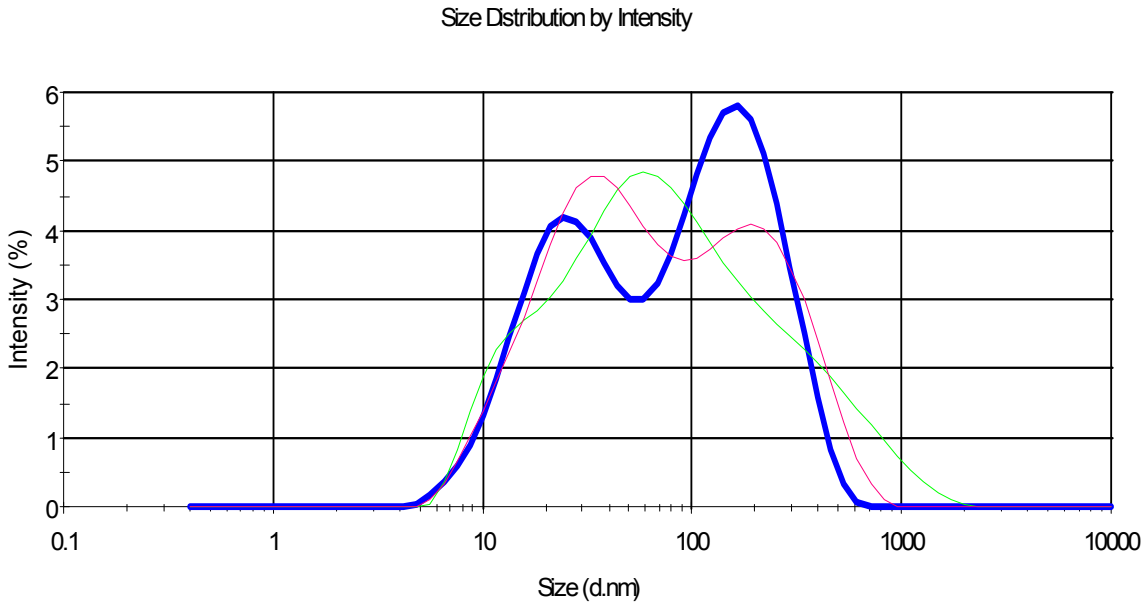

Figure 3.3. Intensity size distribution DLS trace for poly(9-VBA–*co*–DMAEMA) containing 9 mol% 9-VBA

The size distribution by volume DLS trace (Figure 3.4) for poly(9-VBA–*co*–DMAEMA) containing 9 mol% 9-VBA shows that the majority of the copolymer is not aggregating, which is why this composition was initially chosen for further biological analysis.

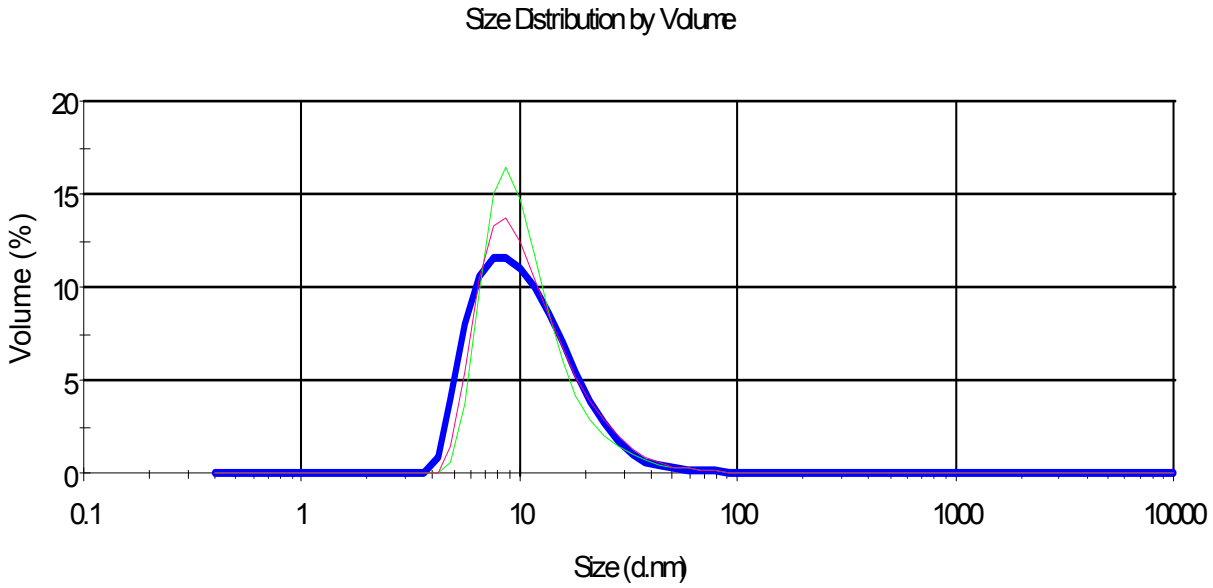

Figure 3.4. Volume size distribution DLS trace for poly(9-VBA–*co*–DMAEMA) containing 9 mol% 9-VBA

Investigation into the various compositions of poly(1-VBT–*co*–DMAEMA) showed results similar to that of poly(9-VBA–*co*–DMAEMA) and the composition containing 9 mol% 1-VBT was also chosen for further biological analysis.

3.4.2 Effect of incorporation of nucleobase-containing groups on cell viability with PDMAEMA

A correlation between high transfection efficiencies and high levels of cytotoxcity is observed for polyelectrolytes such as PDMAEMA. This correlation has led to investigation into non-electrostatic interactions with DNA such as hydrogen bonding. It is predicted that incorporating hydrogen bonding groups will allow for polyplex formation with a decreased cationic character, which contributes to the cytotoxicity according to the proton-sponge hypothesis. The assay utilized in the determination of cell viability with each of the polymer compositions is the MTT assay, which is a colorimetric assay that measures the activity of

enzymes capable of reducing yellow colored MTT (3-(4,5-Dimethylthiazol-2-yl)-2,5-diphenyltetrazolium bromide, a tetrazole) to purple colored formazan (Figure 3.5).

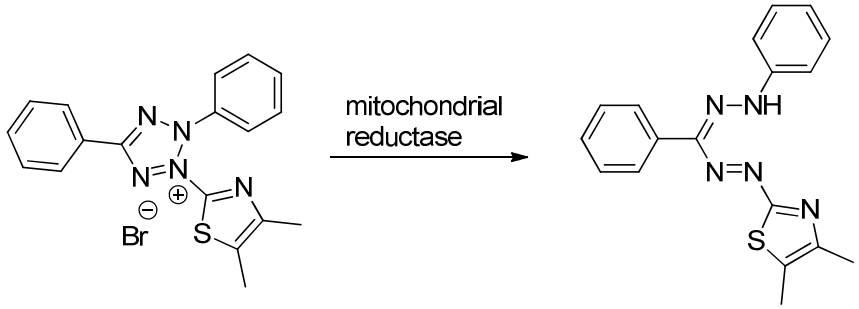

Figure 3.5. MTT scheme

The enzymes capable of reducing MTT to formazan are located within the mitochondria of living cells, so addition of toxic materials would result in increased metabolic dysfunction and a decrease in the amount of formazan produced. The formazan is solubilized upon addition of DMSO and the absorbance of the solution is measured at 570 nm. The polymer concentrations used for the MTT assay ranged from 2-200 μg/mL and one control well, to which no polymer was added, was utilized. Figure 3.6 illustrates the viability of COS-7 as a function of concentration of the three polyelectrolyte compositions. As with the PDMAEMA homopolymer the nucleobase-containing PDMAEMA compositions were highly toxic, showing considerable cell death at a concentration of 20 μg/mL and higher for all three polymer compositions. These results suggest the incorporation of hydrogen bonding groups and reduction of the overall cationic character of PDMAEMA does not affect the cytotoxicity of these vectors, however the ratio of hydrogen bonding groups to protonated amine from PDMAEMA is quite low and could explain why more of an effect was not observed.

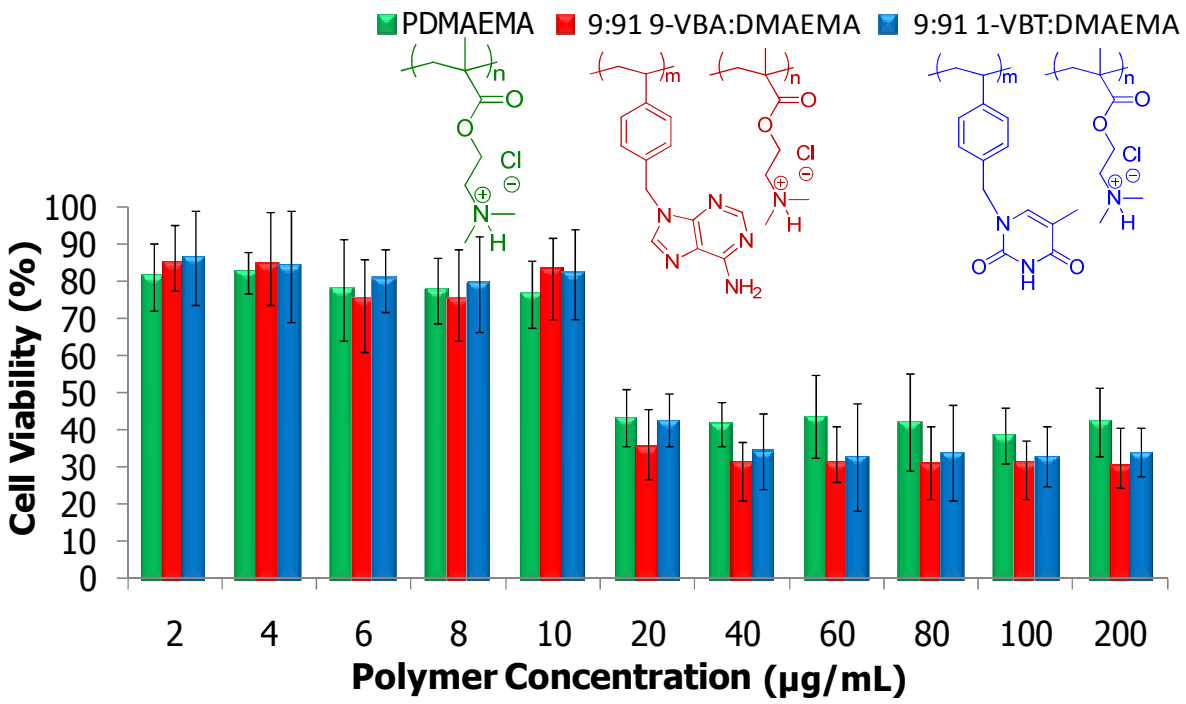

Figure 3.6. MTT assay for COS-7 cells exposed to various concentrations of PDMAEMA and nucleobase-containing PDMAEMA compositions

3.4.3 Effect of incorporation of nucleobase-containing groups on DNA binding efficiency of PDMAEMA

Copolymers of PDMAEMA with hydrogen bonding groups were compared to a PDMAEMA homopolymer to investigate the role of hydrogen bonding in DNA binding efficiency. The hydrogen-bonding copolymers poly(9-VBA–*co*–DMAEMA) and poly(1-VBT–*co*–DMAEMA) and the homopolymer PDMAEMA were dissolved in PBS to form a 1mg/ml solution. DNA binding efficiency was determined by gel shift assays of polyplexes formed at different N/P ratios. Calculation of the N/P ratios was performed using the equation:[15]

$$\frac{N}{P} = \frac{m_p M_{o,D}}{2 m_D M_{o,p}}$$

N/P is the ratio of nitrogen atoms from DMAEMA in the copolymer to the phosphorus atoms in DNA where m_p is the mass of polymer, $M_{o,D}$ is the average repeat unit molecular weight of the plasmid DNA, m_D is the mass of DNA, and $M_{o,p}$ is the molecular weight of the polymer repeat unit. For the copolymers considerations for the polymer repeat unit were made to compensate for the incorporation of non-electrostatic nucleobase components.

The binding efficiency of the various polyelectrolyte compositions was determined using an agarose gel shift assay. The first well was used as a control and no polymer was added to the solution so that the migration of unbound DNA was established. Unbound DNA migrated through the gel and fluoresced downfield from the wells to which the solutions were added. Once bound the DNA was no longer able to migrate through the agarose gel due to both the overall cationic charge of the polyplexes as well as the large size of the complexes. No difference was observed for binding efficiency of the three polymer compositions. Effective DNA binding was determined at an N/P of 1.4 for each polymer as shown in Figure 3.7. One explanation for this observation is that the ratio of hydrogen bonding groups to protonated amine from PDMAEMA was too low to examine the effect of the incorporation of nucleobases.

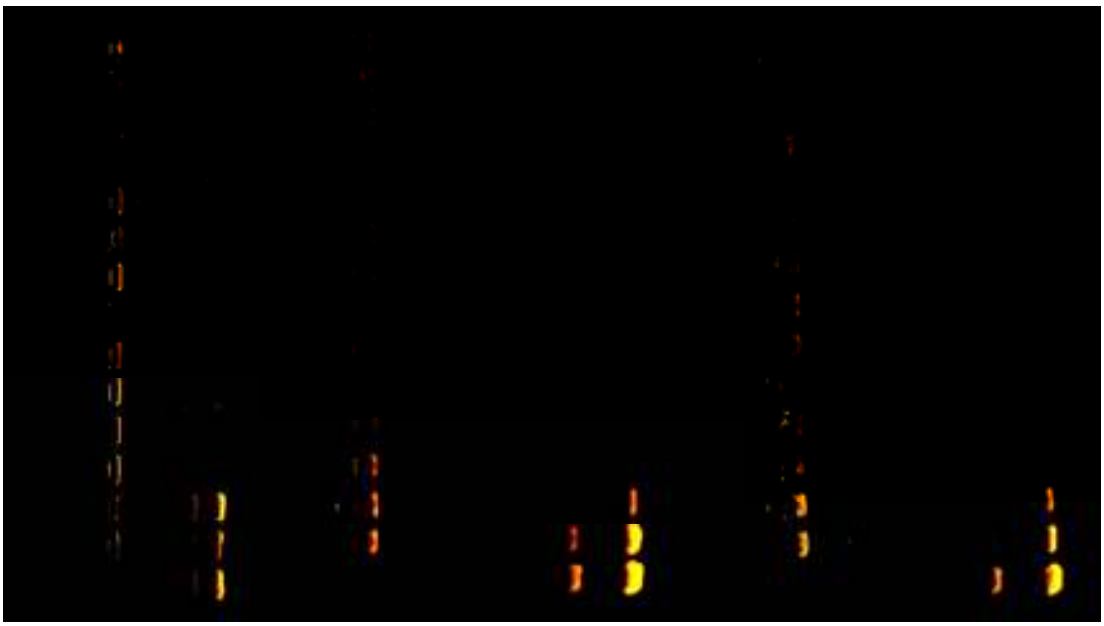

Figure 3.7. Gel shift assay with nucleobase-containing PDMAEMA

3.4.4 Effect of incorporation of nucleobase-containing groups on the gene delivery efficiency PDMAEMA

High transfection efficiencies are achieved using the polyelectrolyte PDMAEMA, however the high level of cytotoxicity observed for this vector has lead to the investigation of the effect of introducing non-electrostatic binding mechanisms to these vectors. The transfection efficiency for nucleobase-containing PDMAEMA was determined to gain a better understanding of the effects of including hydrogen-bonding groups in polyelectrolytes capable of gene delivery. In order to determine the transfection efficiencies of these vectors the Luciferase Expression Assay was utilized. Luciferase is the generic term referring to the class of oxidative enzymes used in bioluminescence. In the Luciferase Expression Assay cells are exposed to a solution of polyplexes formed at various N/P ratios. These cells are incubated with these solutions, allowed to grow further and produce proteins, and then lysed to release the cellular proteins. Solutions

containing these cellular proteins are then analyzed to determine the quantity of luciferase expressed with the cellular machinery.

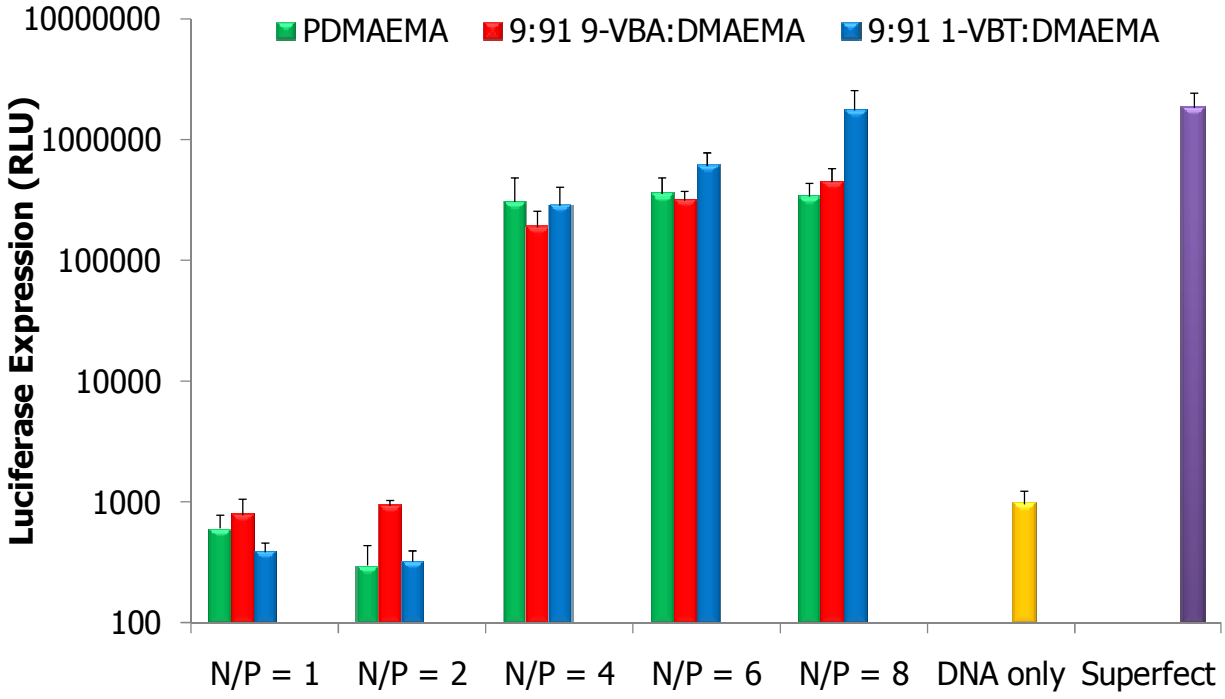

Figure 3.8. Luciferase Expression Assay for nucleobase-containing PDMAEMA

The N/P ratios used for the Luciferase Expression Assay ranged from 1-8 and one control, to which no polymer was added, was utilized. A positive control well was also utilized, in which the gene delivery agent Superfect was added to the DNA solution. Figure 3.8 illustrates the luciferase transfection efficiency to COS-7 as a function of concentration of the three polyelectrolyte compositions. These results suggest the incorporation of hydrogen bonding groups and reduction of the overall cationic character of PDMAEMA does not affect the transfection efficiency of these vectors, however the molar ratio of hydrogen bonding groups to protonated amine from PDMAEMA is quite low and could explain why more of an effect was not observed.

3.5 Conclusions

A series of adenine- and thymine-containing PDMAEMA copolymers were synthesized in order to investigate the effect of the incorporation of nucleobases capable of forming hydrogen-bonding interactions with DNA on non-viral gene delivery. Incorporation of sytrenically linked nucleobases significantly reduced the solubility of PDMAEMA so only copolymers containing low amounts of the nucleobases were able to be analyzed. Results from the MTT cell viability assay, DNA binding gel-shift assay, and the Luciferase Expression gene transfection assay suggest the incorporation of hydrogen bonding groups and reduction of the overall cationic character of PDMAEMA does not affect the cytotoxicity of these vectors, however the ratio of hydrogen bonding groups to protonated amine from PDMAEMA is quite low and could explain why more of an effect was not observed.

3.6 Acknowledgements

We would like to acknowledge Shijing Cheng and Dr. Philippe Bissel for helpful discussions and assistance with monomer synthesis. We would also like to acknowledge Dr. John Layman, Dr. Sean Ramirez, Matthew Green, and Michael Allen for assistance with the various biological assays.

3.7 References

(1) Cherng, J. Y.; vandeWetering, P.; Talsma, H.; Crommelin, D. J. A.; Hennink, W. E. *Pharmaceutical Research* **1996**, *13*, 1038.
(2) Jones, R. A.; Poniris, M. H.; Wilson, M. R. *Journal of Controlled Release* **2004**, *96*, 379.
(3) vandeWetering, P.; Cherng, J. Y.; Talsma, H.; Hennink, W. E. *Journal of Controlled Release* **1997**, *49*, 59.
(4) Sahnoun, M.; Charreyre, M. T.; Veron, L.; Delair, T.; D'Agosto, F. *Journal of Polymer Science Part a-Polymer Chemistry* **2005**, *43*, 3551.
(5) Storm, G.; Van De Wetering, P.; Zuidam, N. J.; Cherng, J. Y.; Talsma, H.; Crommelin, D. J. A.; Hennink, W. E. In *10th Meeting of the NATO-Advanced-Studies-Institute on Targeting of Drugs: Strategies for Gene Constructs and Delivery*; Gregoriadis, G. M. B., Ed. Marathon, Greece, 1999, p 192.
(6) Verbaan, F. J.; Klouwenberg, P. K.; van Steenis, J. H.; Snel, C. J.; Boerman, O.; Hennink, W. E.; Storm, G. *International Journal of Pharmaceutics* **2005**, *304*, 185.
(7) Verbaan, F. J.; Oussoren, C.; Snel, C. J.; Crommelin, D. J. A.; Hennink, W. E.; Storm, G. *Journal of Gene Medicine* **2004**, *6*, 64.
(8) Rejman, J.; Bragonzi, A.; Conese, M. *Molecular Therapy* **2005**, *12*, 468.
(9) van der Aa, M.; Zuidam, N. J.; Storm, G.; Hennink, W. E.; Crommelin, D. J. A. In *7th European Symposium on Controlled Drug Delivery* Noordwijk Aan Zee, Netherlands, 2002, p 269.
(10) Verbaan, F.; van Dam, I.; Takakura, Y.; Hashida, M.; Hennink, W.; Storm, G.; Oussoren, C. *European Journal of Pharmaceutical Sciences* **2003**, *20*, 419.
(11) van der Aa, M. A. E. M.; Huth, U. S.; Hafele, S. Y.; Schubert, R.; Oosting, R. S.; Mastrobattista, E.; Hennink, W. E.; Peschka-Suss, R.; Koning, G. A.; Crommelin, D. J. A. *Pharmaceutical Research* **2007**, *24*, 1590.
(12) Prevette, L. E.; Kodger, T. E.; Reineke, T. M.; Lynch, M. L. *Langmuir* **2007**, *23*, 9773.
(13) Sundaralingam, M. *Int. J. Quantum Chem.* **1977**, 11.
(14) Arnott, S.; Bond, P. J.; Selsing, E.; Smith, P. J. C. *Nucleic Acids Res.* **1976**, *3*, 2459.
(15) Layman, J. M.; Ramirez, S. M.; Green, M. D.; Long, T. E. *Biomacromolecules* **2009**, *10*, 1244.

Chapter 4. Synthesis and characterization of nucleobase-containing *t*-butyl acrylate copolymers

4.1 Abstract

Wide literature precedence exists for polymers containing electrostatic interactions and polymers containing hydrogen bonding motifs, however the combination of electrostatic and hydrogen bonding interactions is not widely investigated in current literature. A series of adenine- and thymine-containing *t*-butyl acrylate copolymers were synthesized to investigate the effect of incorporating hydrogen bonding groups into a anionic polyelectrolyte. Anionic polyelectrolytes containing hydrogen bonding groups are expected to exhibit properties of both classes of supramolecular interactions. The ratio of 9-VBA to *t*-butyl acrylate was determined using both NMR and TGA. Cleavage of the *t*-butyl group allowed for calculation of the molar ratios from the weight loss at 230 ^{o}C as seen in the TGA chromatograph. DSC was utilized in the characterization of the thermal properties of the nucleobase-containing *t*-butyl acrylate copolymers. Cleavage of the *t*-butyl group will give nucleobase-containing copolymers with poly(acrylic acid), which is deprotonated under basic conditions.

4.2 Introduction

A large research effort in the field of supramolecular chemistry focuses on polymers composed of a self-assembled molecular subunits or components through noncovalent interactions.[1-5] Noncovalent intermolecular interactions include hydrogen bonding, metal coordination, hydrophobic interactions, and electrostatic effects.[1] One method of self-assembly that is widely researched is through various hydrogen bonding arrays, including those observed for nucleic acid base pairs.[1-8] The high degree of specificity in the self-assembly process of two strands of DNA with complementary nucleic acid sequences is due to the complementary hydrogen bonding arrays of the various nucleobases.[1] One of the most widely accepted hydrogen bonding motifs between the complementary nucleic acid base pairs, known as Watson-Crick base pairs, form the basis of the double helix structure observed in double stranded DNA.[9,10] Hydrogen bond donors (or acceptors) in diagonally opposite sites result in secondary repulsive forces while a donor and an acceptor provide attractive forces.[4,11-14] In multiple hydrogen bonding arrays the binding motif DDD-AAA maximizes the number of attractive secondary interactions and gives the strongest overall interaction while the ADA-DAD binding motif yields a reduced strength for the overall interaction due to the maximized number of repulsive interactions.[4,11-15] The predictability of interactions between long sequences of nucleic acids makes the utilization of nucleobases for hydrogen binding motifs desirable.[16] This allows great flexibility for the formation of hydrogen bonds between the polymer chains. Hydrogen bonding interactions between nucleobase-functionalized compounds significantly alters the properties of the polymer. The well-defined hydrogen bonding interactions between the nucleobases provide the thermodynamic stability required for the self-assembly of these structures. Side-chain functionalized polymers demonstrate the capability of DNA-like assembly of the polymer chains.

Complexation of side-chain functionalized polymers and nucleobase-functionalized monomers significantly alters the bulk state properties of the polymer.

Electrostatic interactions are another form of noncovalent intermolecular interaction directing supramolecular self-assembly. Polyelectrolytes are a class of polymers that contain a high concentration of repeating units containing ionizable groups which is balanced with a cloud of counterions in solution.[17-19] The electrostatic interactions between these charged groups significantly influence the behavior of these polymers in aqueous solvents. Solution pH and temperature, strength of the ionic interactions and concentration also influence the behavior of polyelectrolytes. The two classes of polyelectrolytes are cationic and anionic and are classified with the charge on the polymeric backbone. Poly(acrylic acid) is deprotonated under basic conditions, yielding poly(sodium acetate), which is an anionic polyelectrolyte. Copolymers with this polyelectrolyte previously reported as being capable of micelle formation and drug delivery.[20-25] The combination of the electrostatic interactions of this polyelectrolyte with a repeating unit containing self-complementary hydrogen bonding interactions is expected to result in materials exhibiting interesting self-association based behavior resulting from both classes of intermolecular interactions.[26]

4.3 Experimental

4.3.1 Materials.

Adenine (99%) was purchased from Aldrich and 4-vinylbenzyl chloride (90%) purchased from Fluka, both were used as obtained. Potassium carbonate (99%) was purchased from Aldrich as

used as obtained. Methanol (99.9%), dimethyl sulfoxide (99.9%), chloroform (99.9%) were purchased from Fisher as used as obtained. *t*-butyl acrylate (99.5%, Fisher) was passed through a neutral alumina column to remove free radical inhibitor. 2,2′-Azobisisobutyronitrile (AIBN, 99%, Sigma-Aldrich) was used as received. Deuterium oxide (D2O, 99.9%, Cambridge Isotope Laboratories) was used as received for all NMR measurements. Ultrapure water was obtained with a Millipore Direct-Q5 purification system. All other solvents were used as received from commercial sources without further purification.

4.3.2 Instrumentation.

^{1}H NMR spectroscopic data was collected in DMF-d_7, DMSO-d_6, and D_2O on a Varian 400 MHz spectrometer. Differential Scanning Calorimetry (DSC) was obtained with TA DSC Instruments under nitrogen at a heating and cooling rate of10 ºC/min. Values from the second heating were reported. Thermogravimetric analysis (TGA) was performed on a TA Instruments TGA under a nitrogen atmosphere at a heating rate of 10°C/min.

4.3.3 Synthesis of 9-(4-vinylbenzyl)adenine.

A previously reported synthetic scheme was followed for the synthesis of 9-(4-vinylbenzyl)adenine.[27] A 250 mL round bottom flask was charged with adenine (10.00 g, 74 mmol), 4-vinylbenzyl chloride (11.41 g, 74.74 mmol), tetramethyl ammonium iodide (44.6 mg, 0.22 mmol), potassium carbonate (13.70 g, 99.16 mmol), and anhydrous DMSO (100 mL). Nitrogen gas was bubbled through the reaction solution for approximately 30 minutes. The

reaction solution was stirred at room temperature for 48 hours. The solution was filtered and precipitated into distilled water. The product was recrystallized from a 1:3 chloroform:methanol solution four times and a white solid was obtained with 34% yield.

4.3.4 Synthesis of poly(9-VBA-co-tBA).

A 50 mL round bottom flask was charged with 9-(4-vinylbenzyl)adenine and *t*-butyl acrylate in varying amounts. The glassware was purged with nitrogen. Anhydrous DMF was added to make a 20 wt% solution. AIBN initiator (0.5 mol%) solution in anhydrous DMF was syringed into the reaction solution. The flask was immersed in an oil bath at 65 ^{o}C and stirred for 24 hours at this temperature. The reaction solution was cooled to room temperature and diluted with an equal volume of chloroform. The resulting solution was precipitated into hexanes and dried overnight at 100 ^{o}C under vacuum.

4.4 Results and Discussion

4.4.1 Synthesis and characterization of nucleobase-containing *t*-butyl acrylate copolymers

The goal was to synthesize a series of nucleobase-containing water-soluble polymers containing various amounts of the hydrogen bonding moieties in order to investigate the effect of the inclusion of the hydrogen bonding groups on thermal and mechanical properties of the resulting polymers.

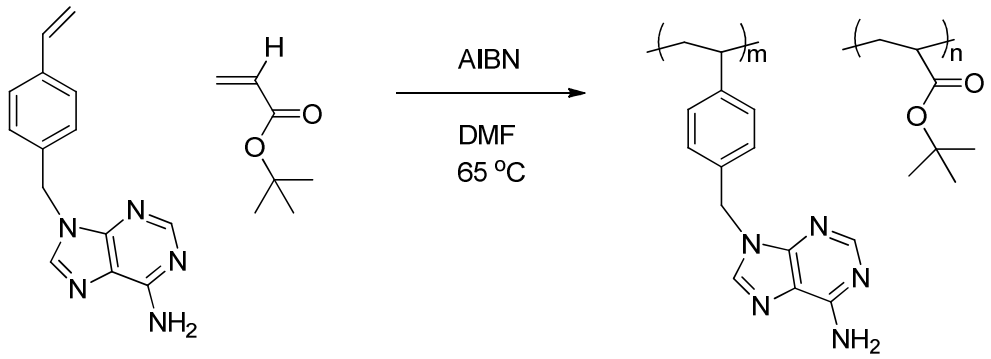

Figure 4.1. Synthesis of poly(9-VBA-co-tBA)

A series of *t*-butyl acrylate copolymers were synthesized due to the ability to perform post polymerization functionalization reactions on these copolymers. The *t*-butyl group is both thermally and chemically labile, allowing a great degree of flexibility in synthetic methods for achieving water-soluble copolymers.

4.4.2 Effect of incorporation of a nucleobase-containing comonomer on the thermal properties of t-butyl acrylate copolymers

The resulting polymers were characterized using TGA and DSC to allow for analysis of the thermal properties before post-polymerization functionalization reactions. The TGA thermograph allowed for quantification of the polymer composition through calculations based on weight loss upon cleavage of the *t*-butyl group at approximately 220 ^{o}C (Figure 4.2).

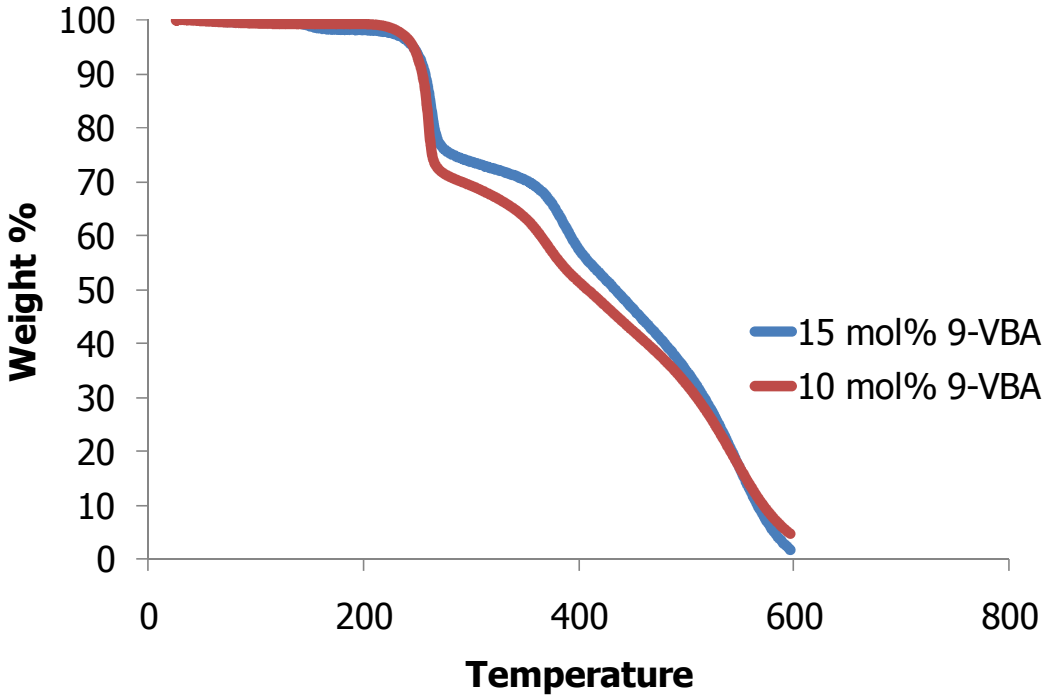

Figure 4.2 TGA of *t*-butyl acrylate copolymers

The weight loss is converted to moles and this value is assumed equal to the number of moles of *t*-butyl acrylate. From this value the weight of *t*-butyl acrylate in the sample is calculated and the remaining sample mass is attributed to the 9-VBA. The values correlating to the mol% 9-VBA from NMR and from TGA and the mol% 9-VBA in the reaction solution are summarized in Table 4.1

Table 4.1. 9-VBA mol%

9-VBA mol% in feed	9-VBA mol% by NMR	9-VBA mol% by TGA
5	9	11
10	13	16
15	22	25
20	36	37

These copolymers were also analyzed using DSC to obtain glass transition temperatures for the series. An increase in the glass transition temperature is observed for poly(9-VBA–*co*–*t*-butyl acrylate) with increased amounts of 9-VBA in the polymer composition. The observed increase in the glass follows the trend defined by the Fox copolymer glass transition equation: $\frac{1}{Tg} = \frac{w_a}{Tg,_a} + \frac{w_b}{Tg,_b}$. In this equation the T_g of the copolymer is calculated from the weight fraction of each monomer and the T_g of each homopolymer. The glass transition temperatures are summarized in Table 4.1.

Table 4.2. Glass transition temperatures for poly(9-VBA-co-tBA)

9-VBA mol%	T_g (^oC)
9	49
13	65
22	67
36	90

4.5 Conclusions

A series of 9-VBA copolymers with *t*-butyl acrylate were synthesized and analyzed using NMR, TGA, and DSC. The ratio of 9-VBA to *t*-butyl acrylate was determined using both NMR and TGA. Cleavage of the *t*-butyl group allowed for calculation of the molar ratios from the weight loss at 230 ^oC as seen in the TGA chromatograph.

4.6 Acknowledgments

We would like to acknowledge Shijing Cheng and Dr. Philippe Bissel for helpful discussions and assistance with monomer synthesis. We would also like to thank Dr. Erin Murphy for helpful discussions.

4.7 References

(1) Cheng, C. C.; Huang, C. F.; Yen, Y. C.; Chang, F. C. *J. Polym. Sci. Pol. Chem.* 2008, *46*, 6416.
(2) Beijer, F. H.; Kooijman, H.; Spek, A. L.; Sijbesma, R. P.; Meijer, E. W. *Angew. Chem.-Int. Edit.* 1998, *37*, 75.
(3) Binder, W. H.; Zirbs, R. In *Hydrogen Bonded Polymers*; Springer-Verlag Berlin: Berlin, 2007; Vol. 207, p 1.
(4) Lawrence, D. S.; Jiang, T.; Levett, M. *Chem. Rev.* 1995, *95*, 2229.
(5) Lehn, J. M. In *Conference on Polymers in the 3rd Millennium*; Polymer Int, I. D., Electr Insulat Soc, I. A. E., Sism, W. I. D., Eds.; John Wiley & Sons Ltd: Montpellier, France, 2001, p 825.
(6) Lutz, J.-F.; Pfeifer, S.; Chanana, M.; Thuenemann, A. F.; Bienert, R. *Langmuir* 2006, *22*, 7411.
(7) Mather, B. D.; Baker, M. B.; Beyer, F. L.; Berg, M. A. G.; Green, M. D.; Long, T. E. *Macromolecules (Washington, DC, United States)* 2007, *40*, 6834.
(8) Sivakova, S.; Rowan, S. J. *Chemical Society Reviews* 2005, *34*, 9.
(9) Hoogsteen, K. *Acta Crystallographica* 1963, *16*, 907.
(10) Sundaralingam, M. *Int. J. Quantum Chem.* 1977, 11.
(11) Jorgensen, W. L.; Pranata, J. *Journal of the American Chemical Society* 1990, *112*, 2008.
(12) Lehn, J. M. In *4th European Polymer Federation Symp on Polymeric Materials*; Huthig & Wepf Verlag: Baden Baden, Germany, 1992, p 1.
(13) Lehn, J. M. In *Conference on the Nato Advanced Research Workshop on Supramolecular Science - Where It is and Where It is Going*; Ungaro, R. D. E., Ed.; Springer: Lerici, Italy, 1998, p 287.
(14) Reinhoudt, D. N.; Stoddart, J. F.; Ungaro, R. *Chemistry-a European Journal* 1998, *4*, 1349.
(15) Krische, M. J.; Lehn, J. M. In *Molecular Self-Assembly* 2000; Vol. 96, p 3.
(16) Sivakova, S.; Rowan, S. J. *Chem. Soc. Rev.* 2005, *34*, 9.
(17) Elkins, C. L.; Park, T.; McKee, M. G.; Long, T. E. *Journal of Polymer Science Part a-Polymer Chemistry* 2005, *43*, 4618.
(18) Layman, J. M.; Ramirez, S. M.; Green, M. D.; Long, T. E. *Biomacromolecules* 2009, *10*, 1244.
(19) McKee, M. G.; Hunley, M. T.; Layman, J. M.; Long, T. E. *Macromolecules* 2006, *39*, 575.
(20) Kilian, L.; Wang, Z. H.; Long, T. E. *Journal of Polymer Science Part a-Polymer Chemistry* 2003, *41*, 3083.
(21) Li, G. Y.; Guo, L.; Ma, S. M. *J. Appl. Polym. Sci.* 2009, *113*, 1364.
(22) Merkel, O. M.; Beyerle, A.; Librizzi, D.; Pfestroff, A.; Behr, T. M.; Sproat, B.; Barth, P. J.; Kissel, T. *Molecular Pharmaceutics* 2009, *6*, 1246.
(23) Sheikh, N.; Jalili, L.; Anvari, F. *Radiat. Phys. Chem.* 2010, *79*, 735.
(24) Singh, B.; Sharma, V. *Int. J. Pharm.* 2010, *389*, 94.
(25) Wu, W. T.; Zhou, T.; Berliner, A.; Banerjee, P.; Zhou, S. Q. *Chem. Mat.* 2010, *22*, 1966.
(26) Deng, L.; Wang, C. H.; Li, Z. C.; Liang, D. H. *Macromolecules* 2010, *43*, 3004.
(27) Srivatsan, S. G.; Verma, S.; Parvez, M. *Acta Crystallographica Section C-Crystal Structure Communications* 2002, *58*, o378.

Chapter 5. Future Directions

5.1 Nucleobase-containing PDMAEMA

Investigation into the reactivity ratios of styrene and DMAEMA using the Mayo-Lewis method and comparing these reactivity ratios to that of 9-VBA and DMAEMA would provide insight into the possible effect the nucleobase has on the reactivity ratios of the two monomers. In addition further analysis of the 9-VBA/DMAEMA polymerization using different IR wavenumbers would confirm the results discussed in chapter 2.

Initial results from solution rheology of a PDMAEMA copolymer containing 9 mol% 9-VBA showed increased viscosity as compared to the PDMAEMA homopolymer. Further investigation into the solution properties of adenine-containing PDMAEMA in aqueous solution is expected to show increased viscosity with increased molar ratio of the hydrogen bonding groups.

Copolymers of 9-VBA and DMAEMA were shown to have salt-triggering effects. Further investigation using these copolymers and varying concentrations of salt solutions would provide further insight into the cloud point, or the salt concentration at which the salt-triggering is first observed.

Further investigation into various biological of these copolymers should gain more insight into the role the nucleobase groups play in gene transfection with cationic polyelectrolytes. It is expected that DNA binding will be achieved using higher molar ratios of both 9-VBA and 1-VBT. The hydrogen bonding interactions are predicted to assist in binding DNA along with the electrostatic interactions of PDMAEMA. In addition the cytotoxicity of the

copolymers should be reduced as the overall cationic character is decreased. It is believed that the cationic character leads to cell death with these cationic gene delivery vectors.

5.2 Synthesis and characterization of nucleobase-containing *t*-butyl acrylate copolymers

Post-polymerization functionalzation of these copolymers will yield a diverse series of copolymers with various characteristics. Converting the acrylate to the deprotonated acrylic acid form would provide nucleobase-containing anionic polyelectrolytes. Comparison of the structure-property relationships of these copolymers to that of the PDMAEMA copolymers would provide interesting insight into the similarities and differences of anionic and cationic polyelectrolytes containing hydrogen-bonding groups.

Investigation into the possible reaction of adenine with a carboxylic acid should demonstrate whether the nucleobase groups are affected during the post-polymerization reaction forming the acrylic acid copolymers.

5.3 Synthesis and characterization of a nucleobase-containing ionene

Step-growth polymerizations allow for the synthesis of a class of polymers known as ionenes. One type of ionene, known as an ammonium ionene, is synthesized from a diamine and a dibromide. The synthesis of nucleobase-containing ionenes is predicted with the synthesis of a nucleobase-containing diamine. Figure 5.1 illustrates the synthetic scheme for this diamine, starting with the reaction of a diamine containing a secondary amine which is fuctionalized using thionyl chloride. This product is then further reacted via a Michael addition reaction with adenine to attach this nucleobase as a pendant group.

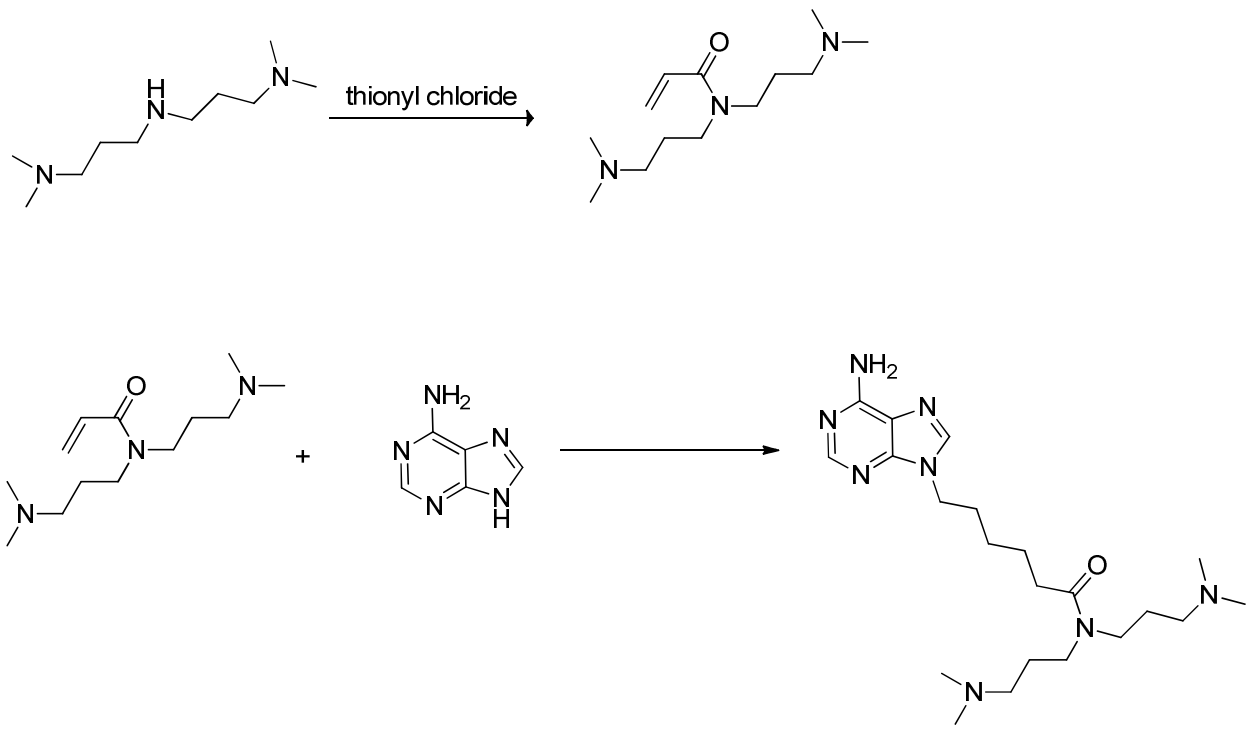

Figure 5.1. Synthesis of a nucleobase-containing diamine

The diamine containing a pendant nucleobase is then reacted with a dibromide to yield a nucleobase-containing ionene (Figure 4.4) . This ionene is predicted to exhibit increased thermal and mechanical properties as with the nucleobase-containing polyelectrolytes previously discussed. Blending of adenine- and thymine-containing ionenes is predicted to allow for hydrogen bonding interactions between polymer chains, which will increase the apparent molecular weight of the systems as well as the thermal and mechanical properties. These thermally-labile interactions can also be utilized to attach various small molecules such as dyes to the ionene structure.